OLGA BEATRIZ BARBOSA MENDES

Assessing the transferability of the Highway Safety Manual crash prediction model for divided rural multilane highways in Brazil

São Calos

2023

Ficha catalográfica elaborada pela Biblioteca Prof. Dr. Sérgio Rodrigues Fontes da EESC/USP com os dados inseridos pelo(a) autor(a).

Mendes, Olga Beatriz Barbosa
M538a Avaliação da transferibilidade do modelo preditivo de colisões do Highway Safety Manual para rodovias multipistas rurais no Brasil. / Olga Beatriz Barbosa Mendes; orientador Ana Paula Camargo Larocca. São Carlos, 2022.

Dissertação (Mestrado) - Programa de Pós-Graduação em Engenharia de Transportes e Área de Concentração em Planejamento e Operação de Sistemas de Transporte -- Escola de Engenharia de São Carlos da Universidade de São Paulo, 2022.

1. Modelo de Previsão de Acidentes. 2. Highway Safety Manual. 3. Transferibilidade. 4. Fator de Calibração Local. 5. Segurança Viária. I. Título.

Eduardo Graziosi Silva - CRB - 8/8907

OLGA BEATRIZ BARBOSA MENDES

Assessing the transferability of the Highway Safety Manual crash prediction model for divided rural multilane highways in Brazil

A thesis submitted in conformity with the requirements for the degree of Master of Science to the Department of Transportation Engineering of the São Carlos School of Engineering, from the University of São Paulo.
Concentration Area: Transportation Systems Planning and Operation.
Tutor: Professor Dr. Ana Paula Camargo Larocca

São Calos
2023

OLGA BEATRIZ BARBOSA MENDES

Avaliação da transferibilidade do modelo preditivo de colisões do *Highway Safety Manual* para rodovias multipistas rurais no Brasil

Dissertação apresentada à Escola de Engenharia de São Carlos da Universidade de São Paulo para obtenção do título de Mestre em Ciências pelo Departamento de Engenharia de Transportes.

Área de Concentração: Planejamento e Operação de Sistemas de Transporte

Orientadora: Profa. Dra. Ana Paula Camargo Larocca

São Calos

2023

FOLHA DE JULGAMENTO

Candidata: Engenheira **OLGA BEATRIZ BARBOSA MENDES.**

Título da dissertação: "Avaliação da transferibilidade do modelo preditivo de colisões do *Highway Safety Manual* para rodovias multipistas rurais no Brasil".

Data da defesa: 01/02/2023.

Comissão Julgadora	**Resultado**
Profa. Associada **Ana Paula Camargo Larocca** **(Orientadora)** (Escola de Engenharia de São Carlos – EESC/USP)	Aprovada
Prof. Dr. **Ali Pirdavani** (Hasselt University/Bélgica)	Aprovada
Profa. Dra. **Karla Cristina Rodrigues Silva** (University of Florida/Estados Unidos da América)	Aprovada

Ana Paula C. Larocca

Coordenador do Programa de Pós-Graduação em Engenharia de Transportes:

Profa. Associada **Ana Paula Camargo Larocca**

Presidente da Comissão de Pós-Graduação:

Prof. Titular **Murilo Araujo Romero**

ACKNOWLEDGMENTS

First and foremost, I express my gratitude to God for providing me with the strength and courage to embark on this journey. I am also deeply thankful to my family, friends, and my fiancé for their unwavering support and love.

I want to extend a special tribute to my beloved mother, who raised me with love and fortitude. She departed this world in 2018, just a year before I began my Master's program. Her accomplishment of earning a master's degree always inspired me, and I feel profoundly honored to be following in her footsteps.

I am immensely grateful to my thesis advisor, Professor Ana Paula Larocca, for her trust in me, for generously sharing her knowledge, and for consistently guiding me in the right direction whenever I needed it.

I also extend my heartfelt appreciation to the experts who played a crucial role in evaluating this thesis and served on my qualification and master's committee: Professor Dr. Ali Pirdavani and Dr. Karla Cristina Rodrigues Silva. Their insights and support were invaluable, motivating me to give my very best.

I would like to acknowledge the dedicated professionals at the Transport Engineering Department, including the esteemed professors who generously imparted their knowledge, as well as the friends I made during this enriching journey, with special thanks to Maria Emília, Mylena, Alanne, and Murilo.

Finally, I would like to note that this study was financed in part by the Coordenação de Aperfeiçoamento de Pessoal de Nível Superior - Brasil (CAPES) - Finance Code 001.

RESUMO

MENDES, O. B. B. **Avaliação da transferibilidade do modelo preditivo de colisões do *Highway Safety Manual* para rodovias multipistas rurais no Brasil.** Dissertação (Mestrado) – Escola de Engenharia de São Carlos, Universidade de São Paulo, São Carlos, 2022.

O método preditivo do *Highway Safety Manual* (HSM) estima a frequência de acidentes aplicando uma função de desempenho de segurança (SPF), em que o fator de calibração estima o ajuste para as condições locais. Para avaliar a transferibilidade em condições diferentes daquelas em que o modelo foi desenvolvido, este trabalho traz uma nova abordagem por meio da avaliação de rodovias brasileiras pedagiadas. Assim, cinco rodovias rurais de multipistas foram segmentadas e avaliadas conforme recomendação do HSM. Para reduzir o problema da subnotificação de dados de acidentes, o método foi desenvolvido para dados de colisões classificados como fatais ou com vítimas (FI) em comparação com os dados totais. O fator de calibração local (Cx) encontrado foi 2,62 para todos os tipos de acidentes e 2,35 apenas para FI. As medidas de avaliação de qualidade de ajuste (*Goodness of Fit* - GOF), foram Desvio Médio Absoluto (MAD), Erro Médio Percentual Absoluto (MAPE), Erro Quadrático Médio (RMSE), R^2 e gráficos de colisões observadas versus estimadas para diferentes cenários. As medidas de GOF para avaliar o desempenho do HSM mostram que a análise com todos os tipos de severidade das colisões apresenta melhor desempenho em comparação ao FI. Por fim, como 2020 foi um ano atípico, em que o tráfego em todo o mundo foi alterado pela pandemia de COVID-19, este estudo teve também como objetivo avaliar a aplicação do modelo de previsão calibrado a uma perturbação real repentina no comportamento do tráfego. O método do HSM foi aplicado para prever colisões em 2020 com o Cx obtido pelos quatro anos anteriores. O resultado foi que para 2020, o $N_{observado}$ foi cerca de 10% inferior ao $N_{previsto}$ calibrado para todos os tipos de acidentes. No entanto, a previsão calibrada de colisões de FI foi muito próxima da contagem observada.

Palavras-chave: Modelo de Previsão de Acidentes. Highway Safety Manual. Transferibilidade. Fator de Calibração Local. Segurança Viária.

ABSTRACT

MENDES, O. B. B. **Assessing the transferability of the Highway Safety Manual crash prediction model for divided rural multilane highways in Brazil.** Thesis (Master) - São Carlos School of Engineering of, University of São Paulo, São Carlos, 2022.

The predictive method presented in the Highway Safety Manual (HSM) estimates the crash frequency by combining a safety performance function (SPF) with crash modification factors (CMFs) and a calibration factor to consider local conditions. This study aims to assess the performance of HSM predictive models when applied to a different condition, such as found on Brazilian roads, by evaluating rural multilane highways. Five divided four-lane highways were segmented and considered following HSM guidelines. To deal with the possible underreporting number of Property Damage Only (PDO) crashes, further investigation was developed for total and Fatal or Injury (FI) severity. Calibration factors (C_x) were calculated, 2.62 for total and 2.35 for FI crashes. The goodness of fit (GOF) tests applied were Mean Absolute Deviation (MAD), Mean Absolute Percentage Error (MAPE), Mean Squared Error (RMSE), R2, and observed versus estimated collisions graphs for different scenarios. The Goodness of Fit measures to assess the HSM performance shows that models for total crashes perform better than FI. Finally, as 2020 was an atypical year in which the COVID-19 pandemic altered traffic patterns worldwide, this study aimed to assess the application of the calibrated prediction model to a sudden disturbance in traffic behavior. The HSM method was applied to 2020 using the C_x obtained from the four previous years. The result showed that for 2020, the observed counts were about 10% lower than the calibrated predictive model estimate of crash frequency for all types of crashes. However, the calibrated prediction of FI crashes was very close to the observed counts.

Keywords: Crash Prediction Models; Highway Safety Manual; Transferability; Local Calibration Factor; Road Safety.

LIST OF FIGURES

LIST OF TABLES

CONTENTS

1 INTRODUCTION

After implementing some of the Decade of Actions for Road Safety (DARS) measures, the number of deaths due to road crashes in Brazil has decreased (F. R. de Andrade & Antunes, 2019). However, the problem persists, causing more than 15 deaths per 100 thousand inhabitants yearly (DATASUS, 2020). This number is about three times higher for emerging countries than developed countries (World Health Organization, 2018). Various factors can contribute to the high number of crashes; thus, data-driven approaches can help identify road safety issues.

Thereat, it is reasonable for nations to develop strategies to improve this situation, involving stricter laws to control the principal risk factors and higher investment in projects and research that advances road safety. Understanding the factors that significantly impact the probability of crashes makes it possible to predict the chances of their occurrence (Hauer, 2004, 2015; Hauer et al., 2012).

Besides, as opposed to the reduction in the total number of people who died on federal highways between 2009 and 2019 (Figure 1), the proportion of fatal crashes in Brazil has increased (Figure 2). Although the increase might be related to the recent crash reporting system changes since 2015 leading to an underreported number of Property Damage Only (PDO) crashes (Brazil Ministry of Justice and Public Security, 2015), further investigation of road safety on Brazilian highways is necessary.

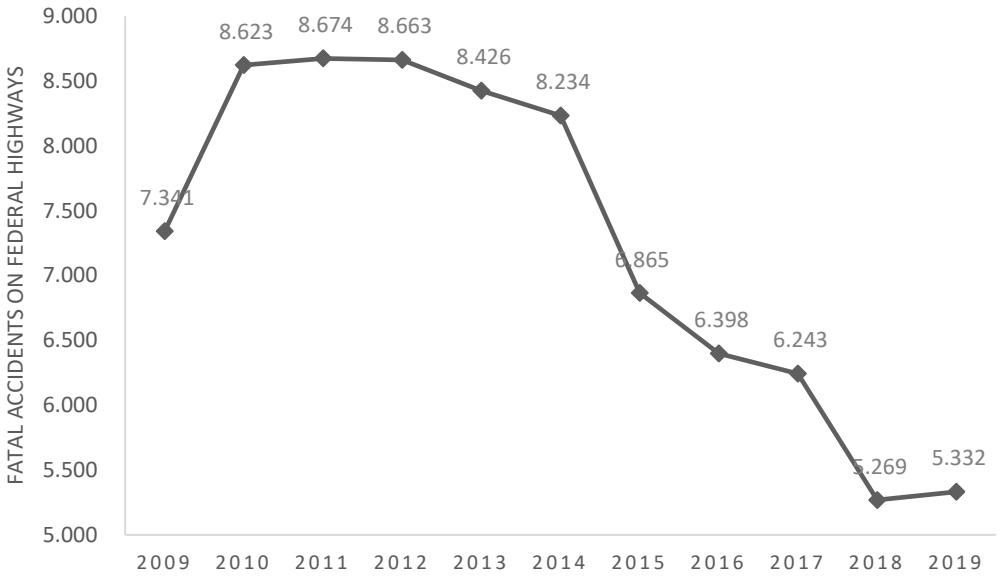

Figure 1 - Number of deaths on Brazilian Federal Highways. Source: Confederação Nacional do Transporte, 2020.

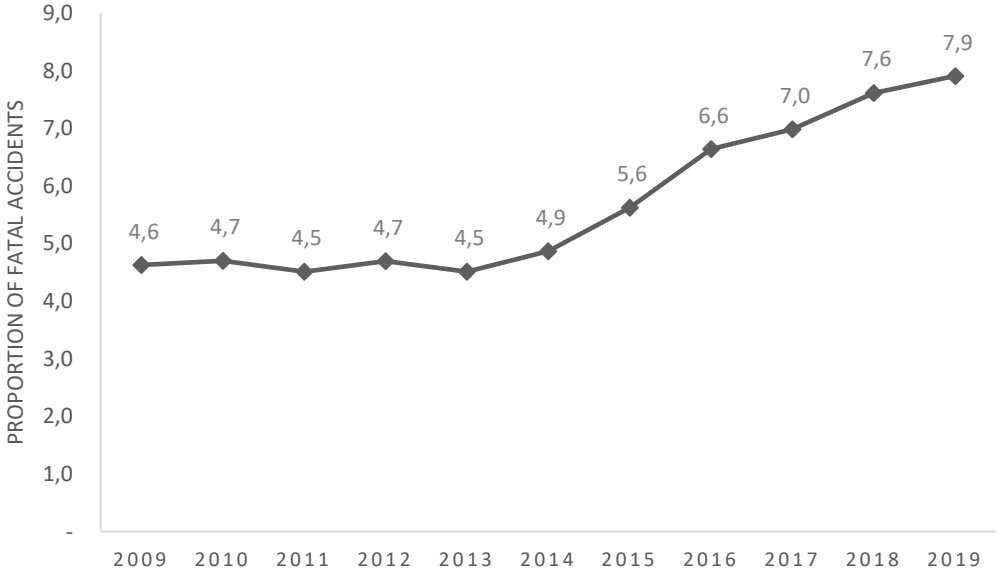

Figure 2 - Proportion of Fatal Accidents Traffic-related in Brazil. Source: Confederação Nacional do Transporte, 2020.

An essential question of how to support decision-makers in evaluating road safety countermeasures arises. Hence, data-driven approaches such as developing Safety Performance Functions (SPF) presented in the Highway Safety Manual (HSM) can help jurisdictions identify crash-contributing factors, especially in places where data is not extensively available, and in the absence of local SPFs (Cunto et al., 2015;

Elagamy et al., 2020; Farid et al., 2016, 2019; Feng et al., 2020; Silva, 2017). Hence, this manuscript aims to assess the transferability of HSM predictive models when applied to an international context, such as on Brazilian highways.

2 LITERATURE REVIEW

2.1 Crash Prediction Models

The crash prediction models presented in the literature generally explain crashes as a consequence of driving performance that does not suit the skills that the road environment demands, either due to traffic flow, geometry attributes, road signs of the route traveled, or vehicular characteristics (Aljanahi et al., 1999; Chang & Mannering, 1999; Geurts & Wets, 2003; Hydén & Várhelyi, 2000; Ivan et al., 1999; Wright et al., 1986). Some of these concepts have been developed over time through the SPF, which are statistical models that estimate the crash rate for a given period or exposure (Abdel-Aty & Radwan, 2000; Buyco & Saccomanno, 1988; Charnes et al., 1982; Hauer, 2004; Lord & Miranda-Moreno, 2008; Oppe, 1979; Quddus, 2008). The statistical analysis methods were first based on studies of risk indicators using only the absolute number, frequency, and crash rate, traditionally defined as determined in Equation 1.

$$\lambda = \mathrm{N} \times \mathrm{p} \tag{1}$$

Where λ is the expected crash number, N is the exposure, and p is the crash rate. While authors such as Foldvary (1979) studied the mean and variance to develop their SPF, Oppe (1979), Ceder & Livneh (1982) obtained models using Multiple Linear Regression (MLR), where the dependent variable related to the rate or number of crashes is a function of variables related to traffic, speed and skid resistance on the pavement. Their analysis achieved reasonable results: the number of single-vehicle crashes tends to decrease as traffic flow increases, while the opposite happens to multiple-vehicle crashes. However, the use of MLR eventually became inadequate to make probabilistic statements.

As Bernoulli's experiment, Poisson regression generated better statistic results for crash prediction. Nevertheless, its limitation is to identify factors that affect each occurrence due to the risk of invalidating test hypotheses because of incorrect confidence limits established in significant parameters (Jovanis & Chang, 1986).

These models evolved to the Poisson log-linear distribution regression, which allows testing the statistical significance of the partial and marginal association

between any combination of categorical factors (Buyco & Saccomanno, 1988). However, this method can lead to overestimation of levels of significance related to regression parameters.

These unsatisfactory properties led researchers to test the Negative Binomial Model (NBM), also called the Poisson-Gamma model, and commonly applied to deal with an overdispersion in the count data. Miaou (1994) used the Maximum Likelihood method to estimate unknown parameters of the model and a mathematical expression that allows a variation to exceed the average. However, the application of NBM and Poisson regression models does not allow the influence of more than one underlying process on the frequency of accidents.

After years of research in this subject, studies began to apply more frequently the Empirical Bayes method to estimate the expected number of crashes at individual sites for one year (Miaou & Lord, 2003). Since then, a question raised by the scientific community has been about small samples, which are common due to the lack of resources to carry out data gathering in some entities of the transport system. This characteristic affects the parameters that the model must have and may have biased results although the distinct advantage of the EB method is that it can be readily applied once a calibrated model is developed (AASHTO, 2010).

2.2 The Highway Safety Model

After the publication of the HSM, evaluating crashes using analytical techniques and tools to quantify the effects that result from decisions in the road network's planning, design, operation, and maintenance was systematized in research-based work. The SPFs found in the HSM were built from negative binomial (NB) regression models using a procedure called generalized linear models (GLM) (Srinivasan et al., 2013) based on the infrastructure and the operational characteristics of the element to be evaluated.

As shown in Equation 2 (AASHTO, 2010), the predicted number of crashes (N_{SPFx}) is the result of an SPF, which is the equation presented for each entity on its base conditions, magnified by a calibration factor C_x and multiple Crash Modification Factors (CMFs). Each CMF reflects the operational and geometric characteristics (y) of an entity (x).

$$N_{predicted} = N_{SPFx} \times C_x \times \left(CMF_{1x} \times CMF_{2x} \times \ldots \times CMF_{yx}\right) \quad (2)$$

The calibration factor (C_x) should be calculated as expressed by Equation 3. The computed C_x is rounded to two decimal places to apply the predictive model.

$$C_x = \frac{\sum_{all\ sites} observed\ crashes}{\sum_{all\ sites} predicted\ crashes} \quad (3)$$

For each facility type and year, it is recommended to calculate correspondent C_x to adjust the model. Replacing default values with locally derived values will improve the reliability of the predictive model. To apply the method, the HSM recommends a set of 30 to 50 sites as a minimum desirable sample representing at least 100 crashes per year (AASHTO, 2010). After the first calibration, the HSM recommends applying the Empirical Bayes (EB) method to provide more reliable results and compensate for the regression-to-the-mean effect.

2.3 Previous work on the transferability of the HSM model

As it has been more than ten years since the first edition of the HSM was published, many researchers have studied the HSM predictive model's impact, transferability, and parameters for different countries. Sun et al. (2013) have stated the challenges, practical solutions, and results of a statewide HSM calibration at rural divided multilane highways in the US. The calibration results indicated that the HSM predicted Missouri crashes reasonably well (C_x = 0.98).

Another study described limitations in applying HSM predictive models for rural two-lane roads in Arizona (Srinivasan et al., 2016). At first, the study highlighted the importance of gathering a larger sample (196 sites, 509 homogeneous segments with about 151 total crashes per year) instead of limiting itself to the HSM's recommendation of 30 to 50 sites with at least 100 crashes per year. Second, it shows the importance of exploring the estimation of calibration functions whenever calibration factors do not fit local data well. The overall calibration factor was 1.079, which is also close to 1.00. It shows that the HSM model has succeeded well for the US cases, as expected.

The calibration factor for other countries, such as Italian motorways, showed that the HSM model ($C_{x,\ not\ calibrated}$ = 1.26) underestimates the observed crash counts (D'Agostino, 2014). La Torre et al. (2019) concluded that applying a jurisdictional-specific base model based on the HSM's SPF represents a solid and reliable tool for practitioners to perform crash prediction for the Italian freeway network.

For Brazilian studies, Rodrigues-Silva (2012) applied the HSM two-lane highways predictive model for the São Paulo state and found a calibration factor of 3.73. Barbosa et al. (2014) developed SPFs for intersections in Belo Horizonte, Brazil, and the calculated C_x was 2.06 following the HSM calibration procedure. Another study for the northeast of Brazil, using Fortaleza city data, found a calibration factor of 0.65. The discrepancy in the result shows how challenging is to develop an SPF that can represent a countrywide model.

The study by Cunto et al. (2015) provided some initial results about the HSM's SPFs for urban roads in Brazil. The data was collected from the urban area of Fortaleza city as well. The C_x for signalized intersections was 0.98, while for stop-controlled intersections was 2.15.

Waihrich & Andrade (2015)investigated the calibration of the HSM predictive method to multilane highways in the state of Minas Gerais (southeast of Brazil) and Goiás (central-west of Brazil), including the Federal District, resulting in a C_x of 2.37 and 1.58 for each studied region, respectively. The results did not confirm the transferability of the original HSM model calibrated according to the studied scenarios, which shows the need for more work on this subject.

Rodrigues-Silva (2017) presented a broad study investigating the transferability between two prediction models for two-lane highways: the HSM method and a local SPF. The HSM's SPF was applied to three different Brazilian regions: São Paulo and Minas Gerais, both in the southeast and Paraná in the south. The calculated calibration factors were 3.67, 3.77, and 2.60, respectively. The conclusions elucidate the lack of parameters to consider a model transferable and a gap in the knowledge for models in other facility types.

Elagamy et al. (2020) used four types of segmentation procedures in Egypt, which affected the performance of the transferred SPFs. Unlike Brazil, the HSM model overestimates the crash occurrence on multilane rural roads in Egypt. Similarly, Matarage & Dissanayake (2020) assessed the HSM for Freeways facilities in

California, Maine, and Washington and used a calibration function tool. They found that the model overpredicted all crashes while underpredicting PDO crashes.

Dadvar et al. (2020) proposed a method that aims to adjust the HSM crash prediction model, mainly because traffic agencies and local jurisdictions need a simple and reliable prediction model that provides a better fit of the data than the use of the HSM calibration method. The study stated that using an incorrect C_x while applying SPFs in the "real world" can misallocate resources. On the other hand, giving local jurisdictions a reasonable C_x would still be a significant step.

That is the justification for the study in Saudi Arabia by Al-Ahmadi et al. (2021), which found C_x values from 0.63 to 0.78 for two multi-lanes rural highway segments. For Saudi Arabia, PDO crashes were better estimated by the HSM SPFs than total and FI crashes. Therefore, it is essential to carry out an in-depth study of the local calibration factors as long as there is an assessment of the quality of the SPFs.

Most researchers agreed that the transferability of a model is linked to how similar the site characteristics are compared to base conditions. In addition, the model must be built by associating regions with the same general characteristics. However, proceeding with its calibration and evaluating its transferability is mainly recommended.

The effectiveness of the local calibration factor as a method for transferring SPFs developed for a particular region or nation is widely discussed in the literature. Yehia et al. (2021) found that the success of the transferability may be influenced by the socioeconomic characteristics and distributions of traffic safety data between the source and target regions. Concerning how traffic flow influences the transferability of SPFs, Farid et al. (2016) demonstrated that the AADT was significant only for single-vehicle crashes. Moreover, Feng et al. (2020) showed that segments with high AADTs have crash characteristics different from those with low AADTs, which would be a warning sign in the transferability process.

For diverse nations such as Brazil, the need to assess the crash prediction model is justified as the hunting for the best tool linking large databases such as crash counts, traffic volume, and infrastructure to support investment planning.

2.4 The goodness of fit measures

In addition to the local calibration factor (C_x), measuring the Goodness of Fit (GOF) of the model is very important to assess how well an SPF developed for a different dataset fits the observed data. Quantifying it to compare different results is essential. The most common measures of forecast accuracy are the Mean Absolute Percentage Error (MAPE) and the Mean Absolute Deviance (MAD). Table 1 shows the region, facility type, and estimated Cx of recent studies in which the HSM was applied to the Brazilian road network. It also shows GOF tests used in the prediction model.

Table 1 - Works of HSM method application in Brazil. Source: Author.

Author	Region	Facility Type	C_x	GOF
Rodrigues-Silva (2012)	SP	Two-lane Rural Highways	3,73	Chi square test and Kolmogorov-Smirnov
Barbosa et al. (2014)	CE	Urban Intersection	0,65 2,06	AIC, R^2 statistic, and CURE plots
Cunto et al (2015)	Fortaleza (CE)	Urban Roads	0,98 2,15	MAD, MAPE, CURE, Pearson χ_p^2statistics and z-score
Waihrich & Andrade (2015)	MG GO/DF	Multilane Rural Highways	2,37 1,58	MAD, MAPE and R^2_{Efron}
Rodrigues-Silva (2017)	SP PR MG	Two-lane Rural Highways	3,67 3,77 2,60	MAD, MAPE, R^2_{Efron}, and CURE plots

In recent studies, the Root Mean Square Error (RMSE) is also often applied to evaluate the prediction accuracy of prediction models (Li et al., 2017; Yao et al., 2021; Yehia et al., 2021). On the other hand, for (Dadvar et al., 2020), the CURE plots may not reveal much due to the sample size.

Since the GOF tests measure how well the predicted and expected crashes were fitted after performing the calibration procedure, the Mean Absolute Deviation (MAD), Mean Absolute Percentage Error (MAPE), Root Mean Square Error (RMSE) and the observed versus predicted graphs were applied. The Mean Absolute Deviation (MAD) indicates the average magnitude of variability of the model (Washington et al., 2005). Where $\hat{Y}_i$ corresponds to the predicted data values, Y_i is observed data values, and n is the sample size.

$$MAD = \frac{\sum_{i=1}^{n} |\hat{Y}_i - Y_i|}{n} \quad (4)$$

The Mean Absolute Percentage Error (MAPE) measures the deviation between observed and predicted values, and it was calculated based on Elagamy et al. (2020) to avoid dividing predicted values by a possible zero observed number of crashes. $\hat{Y}_i$ corresponds to the predicted data values, Y_i is the observed data values, and n is the sample size.

$$MAPE = \frac{\sum_{i=1}^{n} |\hat{Y}_i - Y_i|}{\sum_{i=1}^{n} Y_i} \quad (5)$$

The Root Mean Square Error (RMSE) measures the residuals' standard deviation and how close the data points are to a fitted line. Where $\hat{Y}_i$ corresponds to the predicted data values, while Y_i is to the observed data values, and n is the sample size.

$$RMSE = \sqrt{\frac{\sum_{i=1}^{n} (\hat{Y}_i - Y_i)^2}{n}} \quad (6)$$

2.5 The impact of COVID-19 on traffic safety

The influence of lifestyle changes during the COVID-19 pandemic on traffic safety is being investigated worldwide. During the shutdown period, there was a decrease in traffic flow in the majority of countries affected (Yasin et al., 2021). However, there was a substantial rise in the severity of crashes (Ebrahim Shaik & Ahmed, 2022)

Studies suggest that the Nonpharmaceutical Interventions (NPIs) implemented and the increased percentage of people staying at home could improve pedestrian and cyclist safety while increasing motor vehicle drivers' crash risk (N. Dong et al., 2022). However, the average number of cyclists killed or injured per crash tripled compared to previous years (J. Li & Zhao, 2022).

Unexpectedly, many studies pointed out that substantially decreasing the traffic volume would not improve traffic safety, primarily because of an adverse effect of other risk factors that may lead to injuring or killing someone (Yao et al., 2021). It can be related to the homeostasis effect of risky driving behaviors such as speeding and failing to signal. Besides, crashes involving severe injuries are more likely to happen on

highways (X. Dong et al., 2022). Researchers attributed this phenomenon to increased speeding, emptier traffic lanes, reduced law enforcement, not wearing seat belts, and alcohol and drug abuse (Yasin et al., 2021). Hence, law enforcement mechanisms should focus on preventing these behaviors. (Vanlaar et al., 2021).

Another critical effect during this pandemic was that trip lengths shortened while travel frequency decreased. That would be due to doing activities online as a substitute for physical traveling (Ebrahim Shaik & Ahmed, 2022), changing transportation characteristics, and decreased traffic intensity on the roads since e-commerce has risen.

Finally, sudden disturbances in traffic behavior like this pandemic may broaden the sample for understanding risk factors and SPF applications. Hence, the calibrated HSM SPF for 2020 is compared to the crash data count in 2020 to verify its capacity to assess the impacts of COVID-19 on the highways studied in this work.

3 METHODS

3.1 The HSM crash prediction method for divided roadway segments

The required and desirable site characteristics for calibrating the SPFs for divided rural multilane roadways are described in Table 2.

Table 2 - Data needed to calibrate Part C predictive models by facility type for Rural Multilane Highway Segments. Source: AASHTO, 2010.

Data Element	Data Need		Default Assumptions
	Required	Desirable	
Segment length	X		Need actual data
Average annual daily traffic (AADT)	X		Need actual data
Lane width	X		Need actual data
Shoulder width	X		Need actual data
Presence of Lighting	X		Assume no lighting
Use of automated speed enforcement		X	Base default on current practice
Median width	X		Need actual data

The estimated cash count - N_{spf} - for rural multilane highways depends on the Annual Average Daily Traffic (AADT) for each year by segment and the segment length (L) in miles, as shown in Equation 7. The regression coefficients a and b are presented in the HSM (Table 3).

$$Nspf = e^{(a+b\times\ln(AADT)+\ln(L))} \quad (7)$$

Table 3 - Regression coefficients for four-lane highways in HSM (2010). Source: AASHTO, 2010

Facility type / Severity	a	b	c
4-Lane Total	-9.025	1.049	1.549
4-Lane KABC	-8.837	0.958	1.687
4-Lane KAB	-8.505	0.874	1.740

After obtaining the N_{spf}, it must be multiplied by factors that represent the road features to estimate the $N_{predicted}$. These factors are called Crash Modification Factors - CMFs (Equation 8).

$$N_{predicted} = N_{SPFx} \times C_x \times \left(CMF_{1x} \times CMF_{2x} \times \ldots \times CMF_{yx}\right) \quad (8)$$

The Calibration Factor (C_x) would be the one that represents the regional features of each studied highway. After obtaining the $N_{predicted}$, the EB method should be applied to better estimate the expected number of crashes for a single site (Elvik, 2007), as described in Equation 9.

$$k = \frac{1}{e^{(c + \ln(L))}} \quad (9)$$

Where k is the overdispersion parameter associated with the roadway segment, L is the length of the roadway segment (miles), and c is a regression coefficient used to determine the overdispersion of this model (see Table 3). After defining the k value for every studied segment, the next step is to apply the Site-Specific EB Method, where k is used to obtain the weighted adjustment (w) placed on the predictive model estimate in Equation 10.

$$w = \frac{1}{1 + k \times \left(\sum_{all\ study\ years} N_{predicted}\right)} \quad (10)$$

The final step is obtaining the $N_{expected,}$ as shown in Equation 11. This number represents the final calibrated number of crashes for each segment.

$$N_{expected} = w \times N_{predicted} + (1 - w) \times N_{observed} \quad (11)$$

The sequence of steps that must be followed on the predictive method for rural multilane highways is shown in Figure 3.

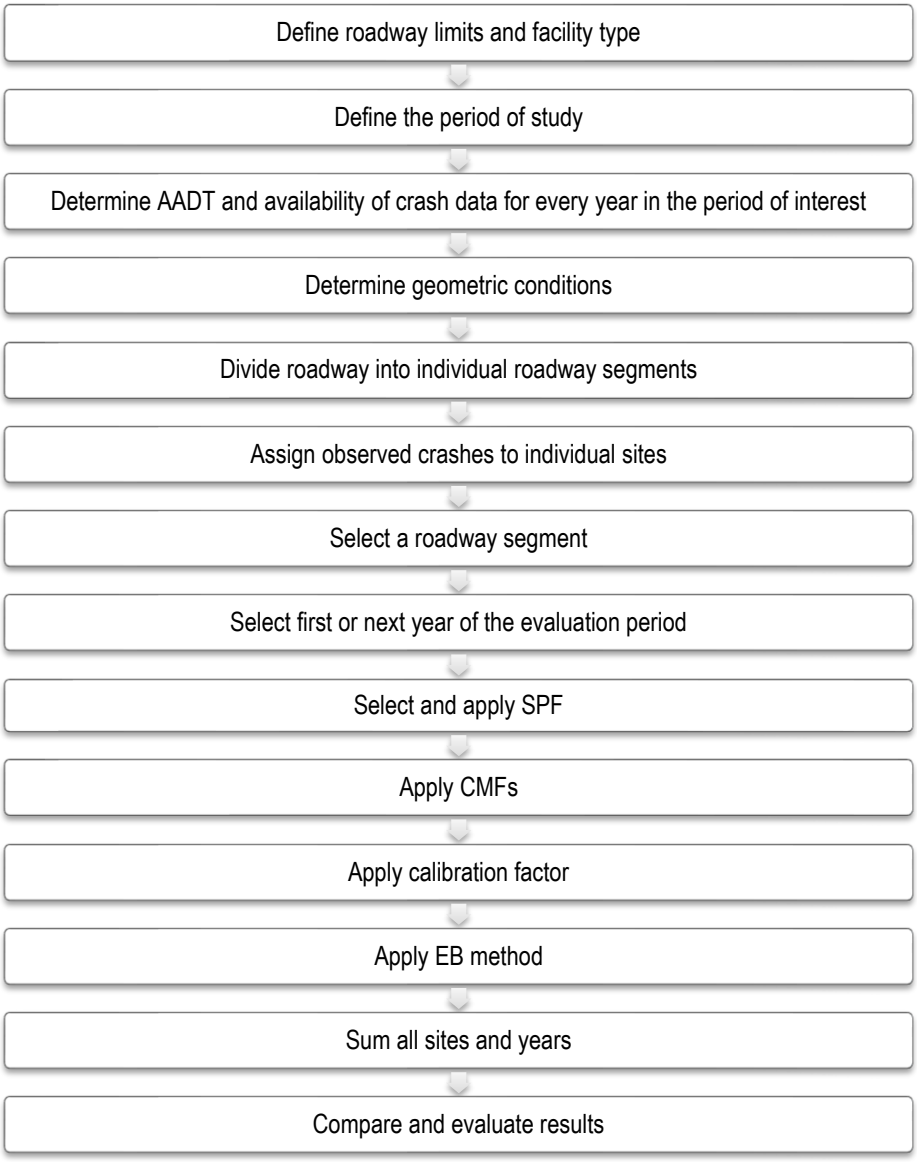

Figure 3 - The HSM predictive method by steps. Source: AASHTO, 2010.

3.2 Road Network Analysis

Five highways in the state of São Paulo managed by toll administration were analyzed. The studied segments are part of the highways SP-255, SP-318, SP-330, SP-334, and SP-345 (Figure 4 and Figure 5). After a road network screening, the sections to be studied were selected based on the geometric aspects and availability of traffic volume information, as presented in Table 4. The length of all the studied roads is 235.6 km. Sensors located at strategic highway points collected the available traffic volume data.

Figure 4 - Location map of the five highways in São Paulo state. Source: Google Earth, 2020.

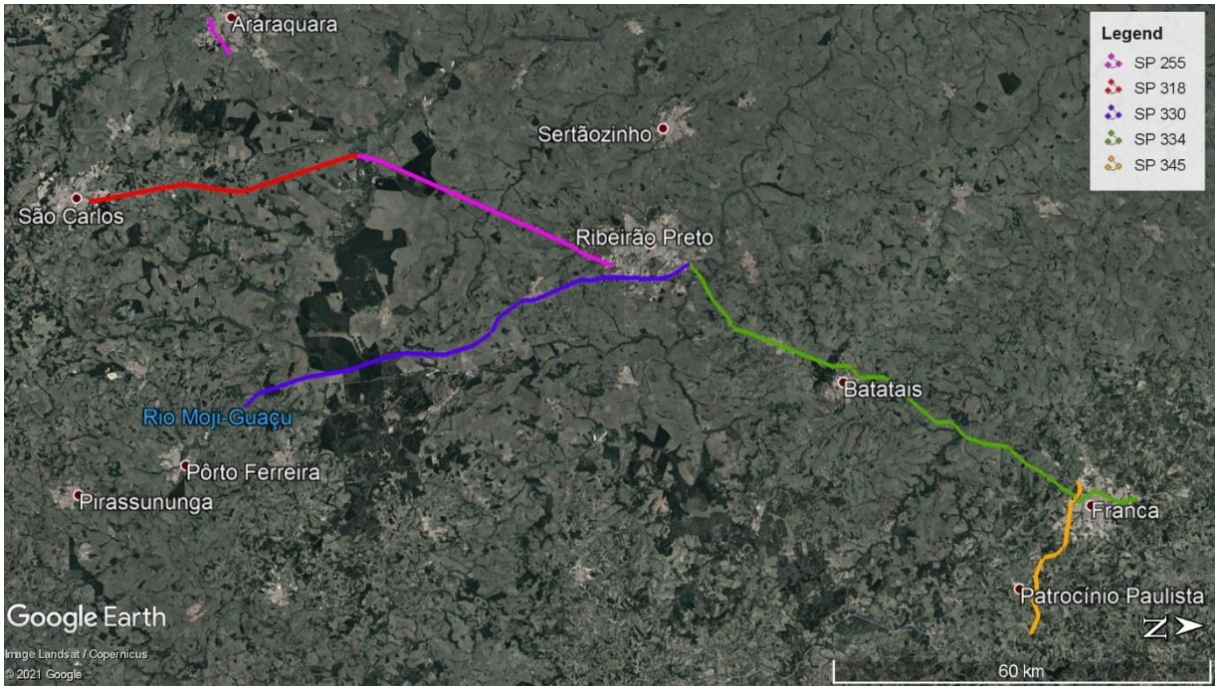

Figure 5 - Map of the five studied highways. Source: Google Earth, 2021.

Table 4 - Main aspects of studied road segments

Highway	ID	Start Point (km)	Endpoint (km)	Length (km)	Observed Crashes (2009 - 2019)	Traffic Volume Data Available				
						2016	2017	2018	2019	2020
SP 255	255_S01	2.8	48.1	45.3	1837	X	X	X	X	X
	255_S02	77.1	83.1	6.0	215	X	X	X	X	X
SP 318	318_S01	235.7	236.1	0.4	24				X	X
SP 330	330_S01	241.0	267.3	26.3	1865		X	X	X	X
	330_S02	267.3	304.0	36.7	3144	X	X	X	X	X
	330_S03	304.0	318.5	14.5	3175	X	X	X	X	X
SP 334	334_S01	319.3	349.5	30.2	2015	X	X	X	X	X
	334_S02	349.5	396.0	46.5	1856	X	X	X	X	X
	334_S03	396.0	406.0	10.0	1237	X	X	X	X	X
SP 345	345_S01	19.4	31.1	11.7	612	X	X	X	X	X
	345_S02	31.1	39.1	8.0	377				X	X

3.2.1 Traffic volume

The traffic volume is detected by sensor devices called "SAT" or "TESC". Their location is shown in Figure 6. The available traffic volume data were verified to match the studied highways.

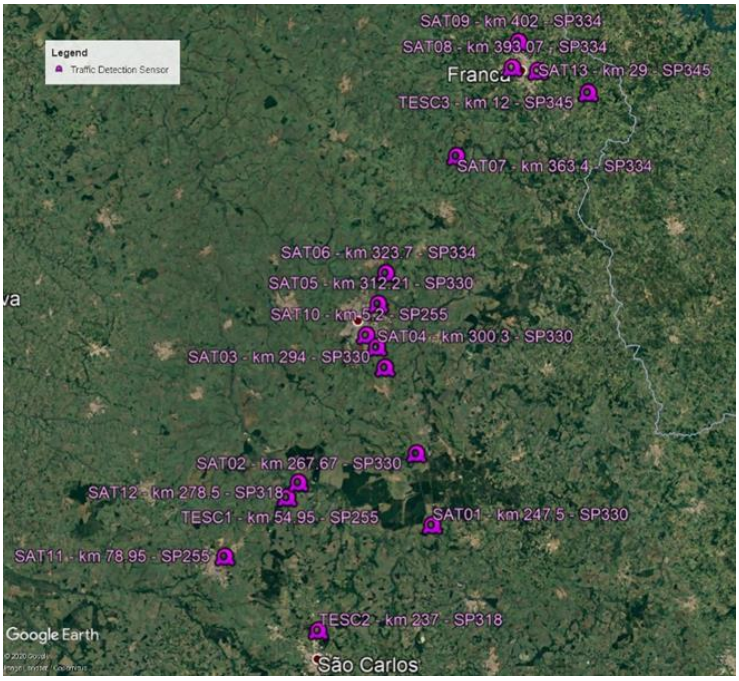

Figure 6 - Location map of Traffic Sensor Devices. Source: Google Earth, 2020.

The Average Annual Daily Traffic (AADT) data was collected for 2016, 2017, 2018, 2019, and 2020, as presented in Table 5 – AADT by study period year. There are a few cases in which there was a lack of information. For SP 318, the available AADT data corresponds to 2019 and 2020 only. As recommended by HSM, the number has been repeated for previous years (2016, 2017, 2018). For SP330_S01, the AADT for 2016 was missing, completed by linear interpolating the existing data.

Table 5 – AADT by study period year. Source: Highway Toll Administration, 2021.

Homogeneous Segments					AADT (veh/day)				
Sensor	**Highway ID**	**Direction**	**Start Point (km)**	**Endpoint (km)**	**2016**	**2017**	**2018**	**2019**	**2020**
SAT10	255_S01	North	48.1	2.8	3173	5725	6049	5969	6374
SAT10	255_S01	South	2.8	48.1	3429	5889	6164	6394	6144
SAT11	255_S02	North	83.1	77.1	6600	5741	6813	6901	6855
SAT11	255_S02	South	77.1	83.1	7972	6602	8357	8461	8498
TESC2	318_S01	North	235.7	236.1	8195	8195	8195	8195	1683
TESC2	318_S01	South	236.1	235.7	8488	8488	8488	8488	1638
SAT01	330_S01	North	241	267.8	9565	9573	9581	9575	8913
SAT01	330_S01	South	267.8	241	8359	9322	9437	9400	8570
SAT04	330_S02	North	267.8	304	10222	13928	13842	13318	12311
SAT04	330_S02	South	304	267.8	27889	13969	13851	13656	12643
SAT05	330_S03	North	304	318.5	28125	29505	19360	30589	29153
SAT05	330_S03	South	318.5	304	27793	29690	19320	31177	29558
SAT06	334_S01	North	319.3	349.5	10535	10985	11682	11090	9764
SAT06	334_S01	South	349.5	319.3	9251	10746	11795	11161	9766
SAT08	334_S02	North	349.5	396	4898	4281	4162	4402	3910
SAT08	334_S02	South	396	349.5	4257	4252	4461	4386	3887
SAT09	334_S03	North	396	406	9284	13758	15524	16283	15655
SAT09	334_S03	South	406	396	7937	14159	14801	15031	13896
SAT13	345_S01	East	31.1	19.4	6402	6750	6689	6692	6548
SAT13	345_S01	West	19.4	31	5469	5666	5541	5788	5748
SAT13	345_S02	East	36	31.1	6402	6750	6689	6692	6548
SAT13	345_S02	West	31.1	36	5469	5666	5541	5788	5748

3.2.2 Homogeneous Segments

The homogeneous segments are portions of the highway with uniform geometric characteristics obtained through the segmentation procedure described in this work, and they are evaluated individually. Figure 7 shows the frequency of a total of 712 segments' length, which presented a greater number of segments with less than one kilometer.

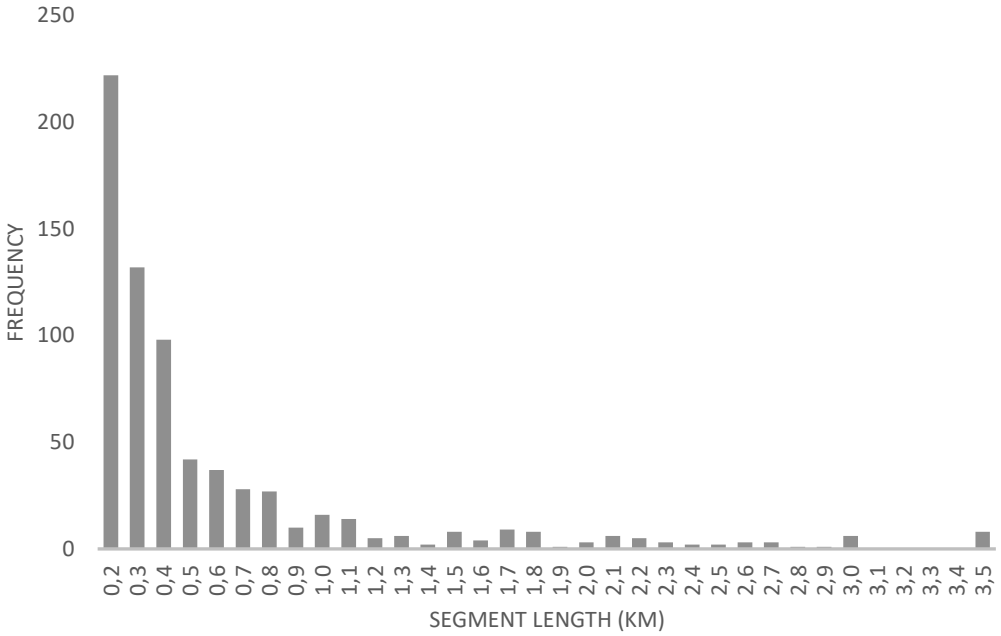

Figure 7 - Frequency of Segment Length. Source: Author.

3.2.3 Crash data

The observed crash data for the study period are presented in Table 6 while Figure 8 shows the crash data analysis by severity.

Table 6 - Main info about observed crash data for the study period.

Severity type	**Total**				**FI**			
Year of Study	**2016**	**2017**	**2018**	**2019**	**2016**	**2017**	**2018**	**2019**
∑	1653	1597	1398	1301	451	467	406	415
Mean	2.32	2.24	1.96	1.83	0.63	0.66	0.57	0.58
Standard deviation	3.47	3.08	2.94	3.08	1.18	1.13	1.13	1.17
Max	33	27	28	39	9	10	7	15
Min	0	0	0	0	0	0	0	0

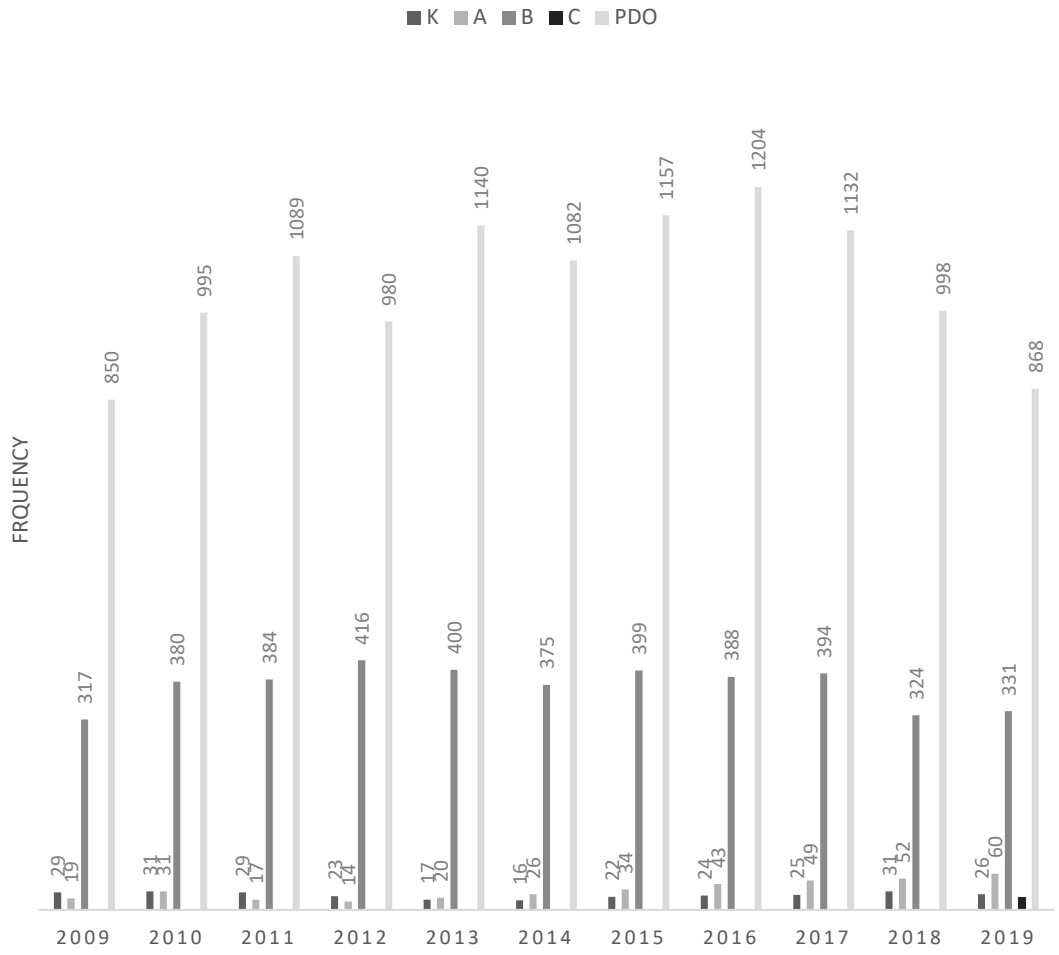

Figure 8 - Crash frequency by severity. Source: DATASUS, 2020.

It supports the idea that KABC[1] data presents lower variation than PDO data since 2015. As expected, the number of PDO crashes has been decreasing since 2015, and this may be related to Brazil's change of regulation for registering PDO crashes, leading to the underreporting problem. Figure 9 and Figure 10 show the characteristics of crashes that occurred on the studied highways.

[1] This is referred to as the KABCO scale: fatal injury or killed (K), incapacitating injury (A), non-incapacitating (B), possible injury (C), and property damage Only (O). The Abbreviated Injury Scale (AIS) was originally developed by the American Association for Automotive Medicine, the Organ Injury Scales (OIS) proposed by the American Association for the Surgery of Trauma and the Injury Severity Score (ISS) used by hospitals.

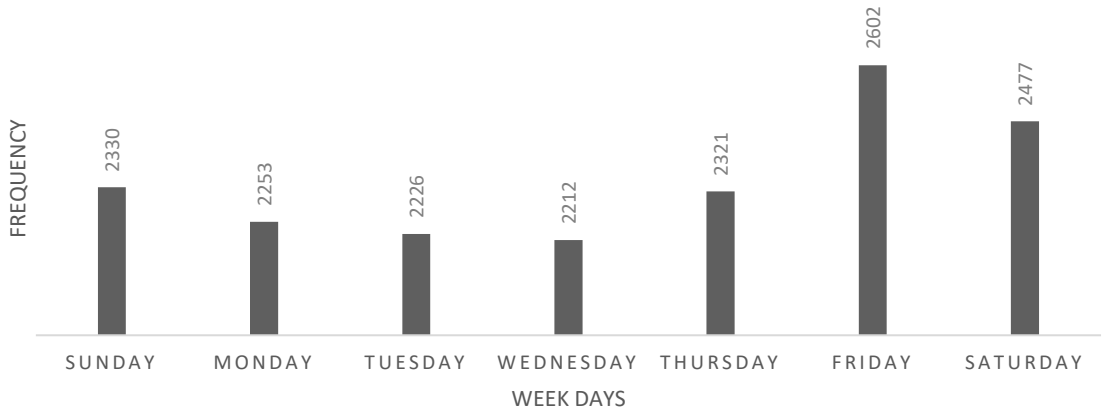

Figure 9 - Crash frequency by week days. Source: DATASUS, 2020.

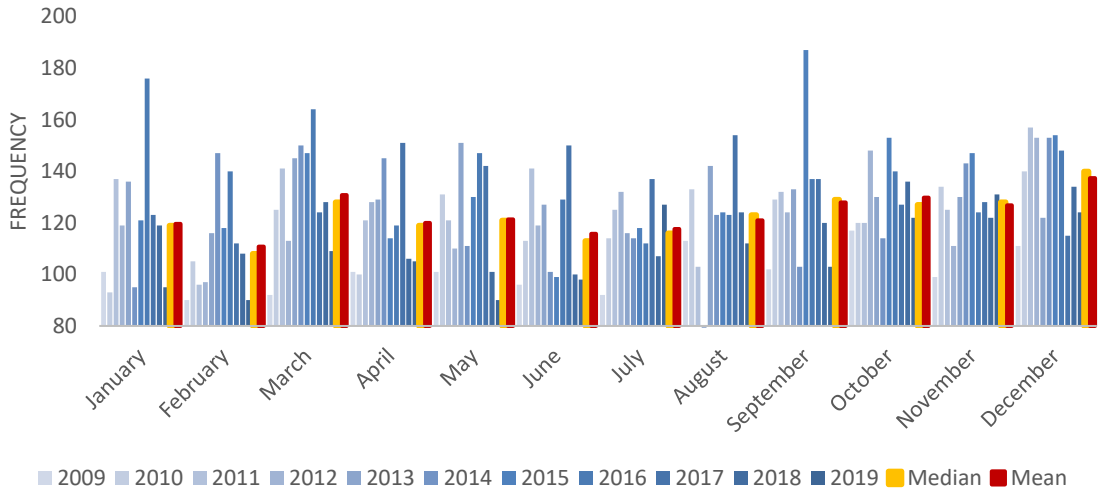

Figure 10 - Crash frequency by month. Source: DATASUS, 2020.

Table 7 presents the proportion of crash data by crash type. It is essential to highlight that this was provided for defining CMFs.

Table 7 – Proportion of crash type for studied highways. Source: Author.

	Collision Type	FI	PDO	Total
	Single vehicle	**0.649**	**0.755**	**0.724**
	Multi-vehicle (total)	**0.351**	**0.245**	**0.276**
Multi-vehicle	Angle	0.037	0.016	0.022
	Head-on	0.011	0.001	0.004
	Rear-end	0.207	0.148	0.165
	Sideswipe	0.073	0.056	0.061
	Other multi-vehicle	0.022	0.025	0.024
	Total Crashes	**1.000**	**1.000**	**1.000**

3.3 Segmentation Procedure

The predictive model for an individual roadway segment or intersection combines an SPF with CMFs and a calibration factor. Therefore, the method is applied to homogeneous segments, to ensure that the ones which have the same characteristics are evaluated as equal. A roadway segment is a portion of the highway that has a consistent roadway cross-section and is defined by two endpoints. A new homogeneous segment begins at the center of an intersection or where there is a change in at least one of the following characteristics of the roadway (AASHTO, 2010):

- Average annual daily traffic (vehicles per day);
- Presence of median and median width (meters[2], rounded widths are recommended as shown in Table 8);

Table 8 - Rounded median width recommended. Source: AASHTO, 2010.

Measured Median Width (m)	**Rounded Median Width (m)**
0.3 ≤ Mw ≤ 4.4	3
4.4 < Mw < 7.4	6
7.4 ≤ Mw < 10.5	9
10.5 ≤ Mw < 13.6	12
13.6 ≤ Mw < 16.6	15
16.6 ≤ Mw < 19.7	18
19.7 ≤ Mw ≤ 22.7	21
22.7 < Mw < 25.8	24
25.8 ≤ Mw < 28.8	27
Mw ≥ 28.8	30

- Shoulder type;
- Shoulder width (meters, rounded widths are recommended as shown in Table 12);

[2] Although the manual recommends foot as unit of length, the most usual in Brazil is meter, which corresponds to around 3,3 feet.

Table 9 - Rounded shoulder width recommended for paved shoulders. Source: AASHTO, 2010.

Measured Shoulder Width (m)	Rounded Shoulder Width (m)
Sw ≤ 0.2	0
0.2 < Sw < 0.5	0.3
0.5 ≤ Sw < 0.8	0.6
0.8 ≤ Sw < 1.1	0.9
1.1 ≤ Sw ≤ 1.4	1.2
1.4 < Sw ≤ 1.7	1.5
1.7 < Sw ≤ 2	1.8
2 < Sw ≤ 2.3	2.1
Sw > 2.3	2.4

- Lane width (meters, rounded widths are recommended as shown in Table 6);

Table 10- Rounded lane width recommended. Source: AASHTO, 2010.

Measured Lane Width (m)	Rounded Lane Width (m)
Lw ≤ 2.8	≤ 2.8
2.8 < Lw < 3	2.9
3 ≤ Sw ≤ 3.1	3.0
3.1 < Sw < 3.3	3.2
3.3 ≤ Sw ≤ 3.4	3.4
3.4 < Lw < 3.6	3.5
Lw ≥ 3.6	3.6

- Presence of lighting;
- Presence of automated speed enforcement.

The segmentation procedure aims to form a database with all possible individual homogeneous roadway segment data. In this study, the spreadsheet was formed by analyzing an orthogonal projection of the road (Figure 11) sent by the highway toll administration.

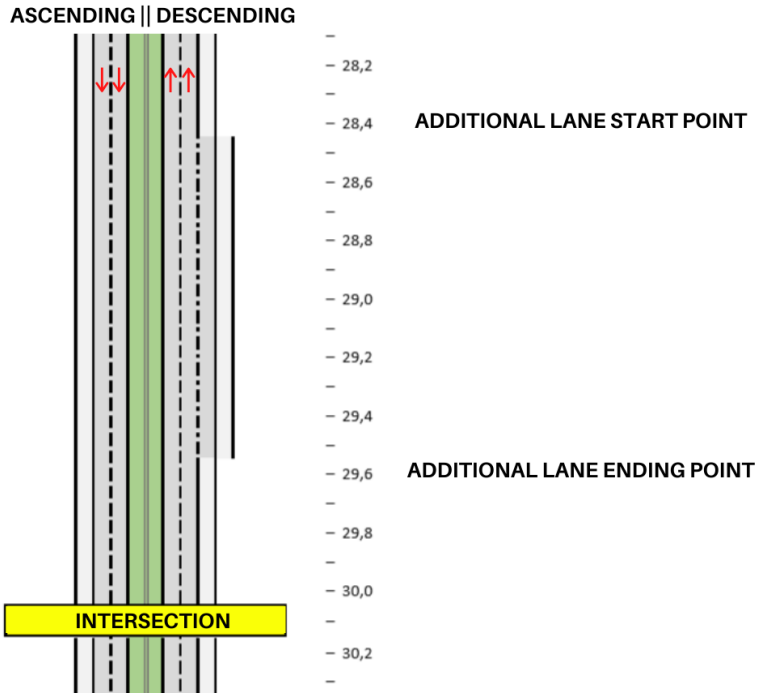

Figure 11 - Orthogonal projection of the Highway SP 255

.

However, it could be considered biased by the lack of geometric design and traffic control information. Then it was necessary to complement the method through verification of the kilometric markers KMZ available (Figure 12) at Google Earth Pro.

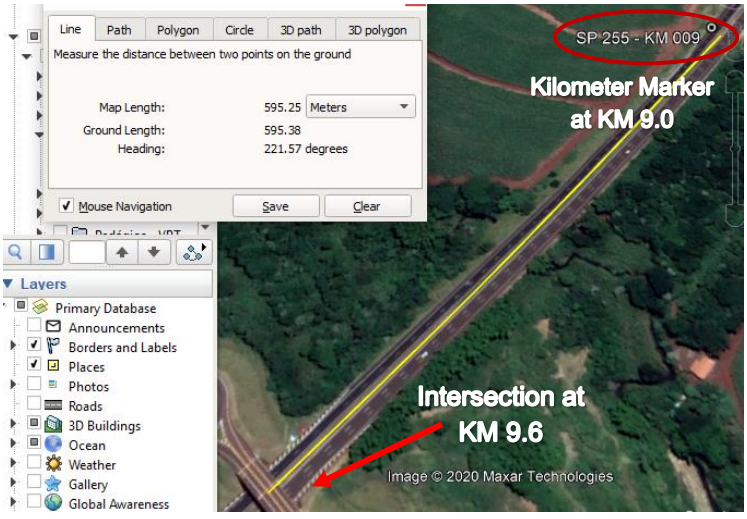

Figure 12 - Segments characteristics verification procedure at Google Earth Pro

In most Brazilian crash reports, no field allows the reporting officer to designate the crash as intersection-related. Once the HSM predictive model has been developed to estimate crash frequencies separately for each site, either a segment or an intersection, it is very important to indicate and exclude from this study those

occurrences related to intersections. Therefore, to assign the crash to an intersection, the following steps based on (ANDRADE; SETTI, 2011), and on the guidance in the HSM were followed:

- Rear-end collisions that happened from 200 meters distance before the off-ramp to 200 meters after the on-ramp of each intersection.
- Collisions that indicate improper traffic control at the intersection.

In addition, Brazil's multilane highways usually have U-turn highway ramps at some points. For this study, all the U-turn elements are overpass bridges, but it is not considered an intersection (Figure 13). Once there was not enough segment sample to study the U-turn highway ramps, they were considered as part of the homogeneous segments. It is recommended to have a sample large enough to study the device for future work.

Figure 13 - U-turn highway ramps overpass bridge

3.4 Crash Modification Factor for Divided Roadway Segments (CMFs)

The CMFs are multiplicative factors used to calculate the predicted number of crashes based on each road feature (Equation 9). The base conditions for each SPF mean that the CMF value is 1.0.

$$N_{predicted} = N_{SPFx} \times C_x \times \left(CMF_{1x} \times CMF_{2x} \times \ldots \times CMF_{yx}\right) \quad (9)$$

For divided roadway segments on rural multilane highways, the default value for base conditions is 12 feet for lane width, 8 feet for the right-hand side shoulder width, 30 feet for median width, no lighting, and no automated speed enforcement. A CMF greater than 1.0 means an expected increase in crashes due to specific road characteristics. At the same time, a CMF value of less than 1.0 indicates an expected reduction in the number of crashes.

3.4.1 CMF_{1rd} – Lane width on Divided Roadway Segments

$$CMF_{1rd} = (CMF_{RA} - 1.0) \times p_{RA} + 1.0 \quad (10)$$

Where:

CMF_{1rd} is the crash modification factor for total crashes;

CMF_{RA} is the crash modification factor for related crash types (run-off-the-road, head-on, and sideswipe), presented in Table 11; and

p_{RA} is the proportion of total crashes constituted by related types of crashes.

Table 11 - CMF for Collision Types Related to Lane Width (CMF_{RA})

Lane Width		**Annual Average Daily Traffic (AADT) (veh/day)**		
ft	**m**	**<400**	**400 to 2000**	**>2000**
9	2.7	1.03	1.03 + 1.38 x 10^{-4} (AADT-400)	1.25
10	3.0	1.01	1.01 + 8.75 x 10^{-5} (AADT-400)	1.15
11	3.4	1.01	1.01 + 1.25 x 10^{-5} (AADT-400)	1.03
12	3.7	1.00	1.00	1.00

The default value of p_{RA} is 0.50, however, the HSM recommends the value to be updated based on local data, which in this study was calculated and found to be 0.47 for the total number of crashes and 0.36 for KAB only (Table 12).

Table 12 - CMF1rd related type of crash proportions to calculate p_{RA}

	Number of crashes			Proportion of crashes		
Collision Type	**KAB**	**PDO**	**Total**	**KAB**	**PDO**	**Total**
Run off Road	1328	5307	6635	0.28	0.46	0.40
Head-on	53	9	62	0.01	0.00	0.00
Sideswipe	347	665	1012	0.07	0.06	0.06
CMF1rd related (∑)	1728	5981	7709	0.36	0.52	0.47
Total Crashes	4814	11607	16421	1	1	1

3.4.2 CMF_{2rd} – Right Shoulder Width on Divided Roadway Segments

The SPF base condition for the right shoulder width variable is 8 ft, which is about 2.44m. The recommended values of CMF for different shoulder width values are presented in Table 13.

Table 13 - CMF for Right Shoulder Width on Divided Roadway Segments (CMF_{2rd}).

Average Shoulder Width		**CMF2rd**
ft	m	
0	0.00	1.18
2	0.61	1.13
4	1.22	1.09
6	1.83	1.04
8	2.44	1

3.4.3 CMF_{3rd} – Median Width

The HSM recommends a CMF value available in Table 14 for the Median Width effect on collision. The CMF value for segments with traffic barriers of any type (either rigid or flexible barrier) is 1.0.

Table 14 - CMFs for Median Width on Divided Roadway Segmnts without a Median Barrier (CMF_{3rd}).

Median Width		**CMF_{3rd}**
ft	m	
10	3.05	1.04
20	6.10	1.02
30	9.14	1
40	12.19	0.99
50	15.24	0.97
60	18.29	0.96
70	21.33	0.96
80	24.38	0.95
90	27.43	0.94
100	30.48	0.94

3.4.4 CMF_{4rd} - Lighting

The equation below presents the value for CMF_{4rd} for lighted segments only. The unlighted segments are considered the SPF base condition, which means the value is 1.0.

$$CMF_{4rd} = 1 - \left[\left(1 - 0.72 \times p_{inr} - 0.83 \times p_{pnr}\right) \times p_{nr}\right] \quad (11)$$

Where:

CMF_{4rd} is the crash modification factor for the effect of lighting on total crashes;

p_{inr} is the proportion of total nighttime crashes for unlighted roadway segments that involve a fatality or injury;

p_{pnr} is the proportion of total nighttime crashes for unlighted roadway segments that involve property damage only; and

p_{nr} is the proportion of total crashes for unlighted roadway segments that occur at night.

In the studied highway there was found similar proportions compared to the HSM recommended values (Table 15).

Table 15 - Proportion of nighttime crashes to calculate p_{inr}, $p_{pnr,}$ and p_{nr}.

	Total	Proportion	PDO	Proportion	FI	Proportion
Nighttime	7376	**0,449**	5138	**0,697**	2226	**0,302**
Total	16421	1,000	11607	0,707	4814	0,293

The locally derived values presented in Table 16 replaced the default values presented in Equation 11 to calculate CMF_{4rd}, as recommended by the HSM.

Table 16 - Nighttime Crash Proportions for Unlighted Roadway Segments.

	HSM	Locally derived values
p_{inr}	0.323	0.302
p_{pnr}	0.677	0.697
p_{nr}	0.426	0.449

3.4.5 CMF_{5rd} – Automated Speed Enforcement

As in the CMF4rd, the base condition of this CMF is where there is no Automated Speed Enforcement. The HSM recommends that the segments with fixed cameras or the sites where the driver cannot be sure if there is an automated speed enforcement should have CMF5rd value of 0.83 for FI accidents and 0.94 for all the types of occurrences.

4 RESULTS AND DISCUSSIONS

This work applied the predictive methodology recommended in Part C in Chapter 11 of the HSM 1st edition. The procedure consists of the method presented in item 3.1 for obtaining N_{spf} for each segment based on its AADT and Length. The CMFs presented in section 3.4 are multiplied as expressed in Equation 1 for each segment, and the result would be the combined $N_{predicted}$. After that, the calibration factor C_x was obtained through the ratio of the observed number of crashes ($N_{observed}$) and the predicted number of crashes ($N_{predicted}$), as expressed in Equation 3.

4.1 The local calibration factor (C_x)

The C_x was estimated separately for 2016, 2017, 2018, and 2019 and once more for the four years combined. The number of cashes obtained through the EB method is called $N_{expected}$. Table 17 shows $N_{observed}$, $N_{predicted}$, $N_{expected}$, and C_x for total and FI crashes. The HSM assumes that the closer the local calibration factor is to 1.0, the more similar the road networks are to the condition for which the model was developed. Thus, the FI C_x compared to the total crashes C_x shows it has performed closer to the HSM model. Still, the value of C_x=2.62 for total crashes and C_x=2.35 for FI crashes shows similarities to Waihrich & Andrade (2015), which found C_x=2.37 for the state of Minas Gerais. To have a better insight, measuring how well the predicted points fit the observed data is necessary.

Table 17 - Main information about $N_{predicted}$, $N_{expected}$ (EB), and C_x.

	Severity	2016	2017	2018	2019	Four-years
Observed Crashes	Total	1653	1597	1398	1301	5949
	FI	451	467	406	415	1739
Predicted Crashes ($N_{predicted}$)	Total	565	570	545	587	2267
	FI	182	186	181	191	741
Expected Crashes (EB) ($N_{expected}$)	Total	1622	1581	1402	1298	5892
	FI	457	472	420	422	1774
C_x	Total	2.92	2.80	2.57	2.22	2.62
	FI	2.47	2.50	2.24	2.17	2.35

4.2 The Goodness of Fit (GOF) Measures

The GOF tests measure how well the predicted and expected crashes were fitted after performing the calibration procedure. The GOF used were Mean Absolute Deviation (MAD), Mean Absolute Percentage Error (MAPE), Root Mean Square Error (RMSE), and the observed versus predicted graphs. For the GOF parameters presented, the smaller the value, the better the model fit. The results are shown in Table 18.

Table 18 - Goodness of Fit of the HSM predictive model by MAD, MAPE, and RMSE tests.

Goodness of Fit Test	Calibrated Predicted Crashes			Expected Crashes		
	MAD	MAPE	RMSE	MAD	MAPE	RMSE
Total	4.44	53%	8.59	0.80	10%	1.33
FI	1.92	78%	3.38	0.86	35%	1.35

As expected, after applying the EB method, the estimated values fit the observed values quite well. The MAD, MAPE, and RMSE show that for the final step, after the EB application, the total crash model performs better than FI.

On the other hand, the values found for MAD and RMSE indicate that the variation of calibrated predicted values is more significant when including PDO crashes, which is reasonable once FI represents a smaller sample (about only 30% of the total crash data). The MAD for FI was 43% of the MAD for total crashes, while for the RMSE, it was 39%. Besides, Waihrich & Andrade (2015) found a value of 5.54 for the MAD for total crashes in the Minas Gerais state, which is 24% greater than the MAD value found for total crashes in the São Paulo state (MAD=4.44).

The results for MAPE indicate that the FI crashes have more prediction errors, which might be explained by the significant difference between total and FI crash counts. Another aspect to highlight is the change in the MAPE calculation (Equation 5), which was adapted to avoid situations where it could be divided by zero. This was because, in the original equation, the term $\hat{Y}_i - Y_i$ is divided by the observed crashes by segment (eventually, no crash happened at some points).

The following graphs show the results of the whole study period. Figure 14 compares the calibrated $N_{predicted,}$ and the observed total and FI crashes to the centerline. The model's output closer to the centerline is considered more reliable as

the predicted data is closer to the observed data. Therefore, it highlights the dispersion of total crashes compared to FI crashes. Also, points below the centerline indicate that the model underestimates the observed data, while points above the centerline signify the overestimation of the observed data.

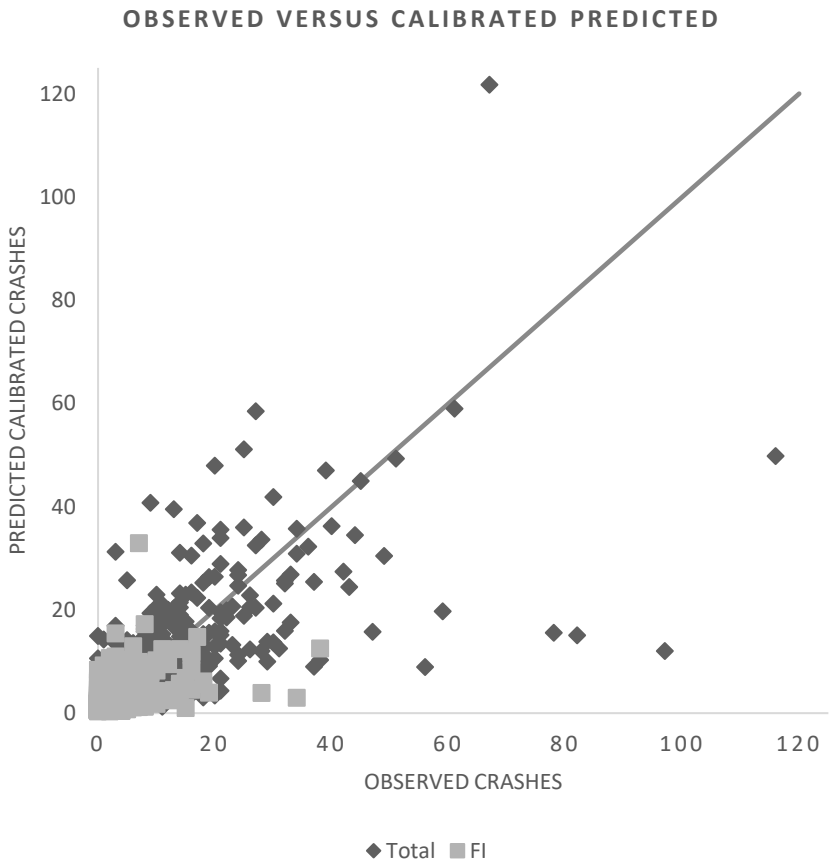

Figure 14 – The correlation of calibrated $N_{predicted}$ versus $N_{observed}$ comparing total and FI crashes for the total period of study.

Figure 15 shows the performance of the predicted values compared to observed data. About 56% of them are under the centerline trend, which suggests that the model has underpredicted most of the data. This underestimation highlights the lack of conformity between the model output and the Brazilian data. The greater the number of observed crashes in a specific segment and year, the clearer the underestimation becomes in the graph.

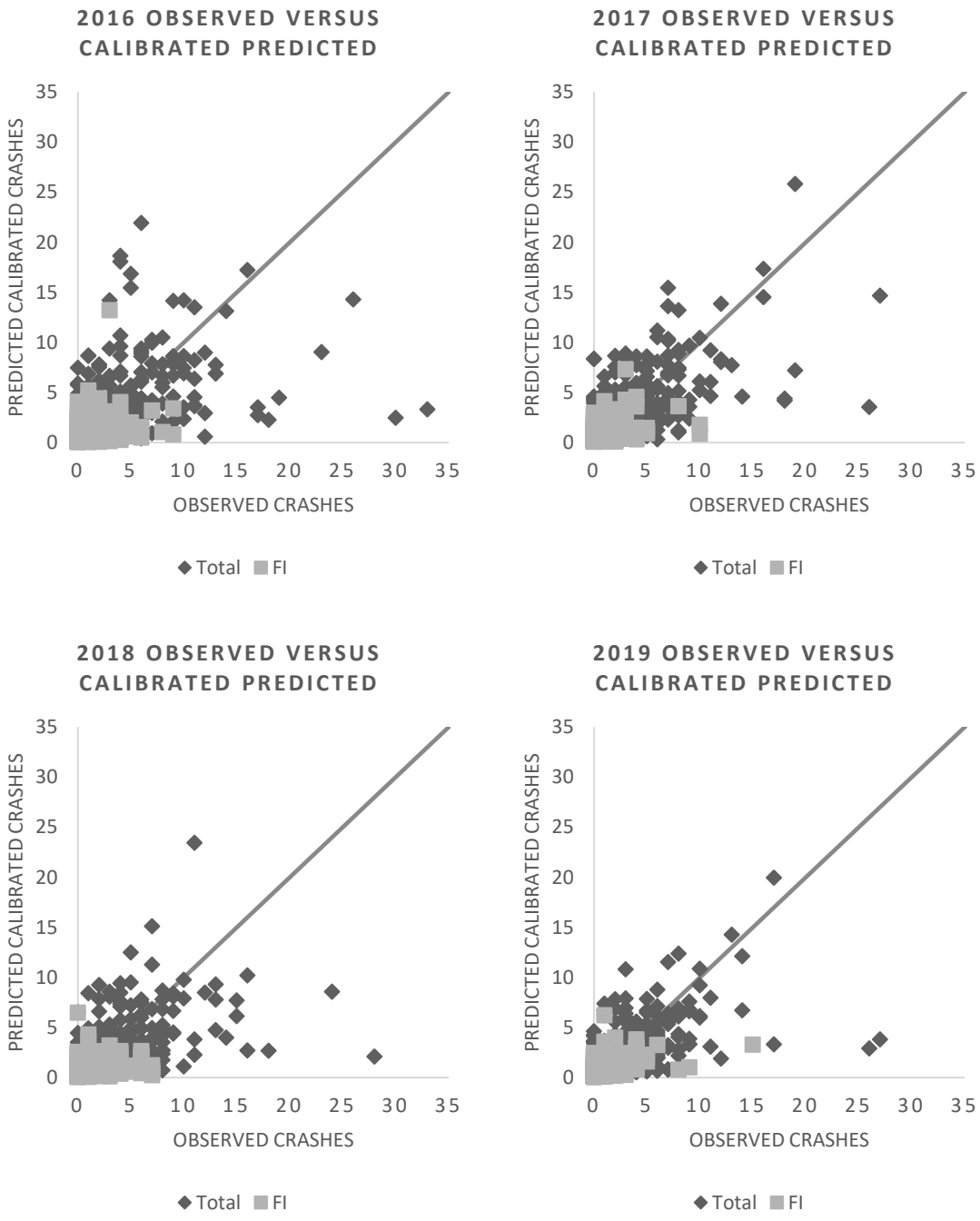

Figure 15 – Comparison between $N_{predicted}$ versus $N_{observed}$ for total and FI crashes for 2016, 2017, 2018, and 2019, respectively.

Figure 16 also compares the calibrated $N_{predicted}$ total and FI crashes to the centerline for each study year. The model's output following the centerline is considered more reliable since the observed data is closer to the predicted data. The graphs have a similar behavior: above the centerline, the points seem denser and closer to the centerline, while under the centerline trend, they seem loose. This

indicates that the overpredicted points are usually closer to matching the observed points than the underpredicted ones.

The following graphs illustrate the difference between $N_{predicted}$ and $N_{expected}$ (i.e., results of the EB application). Figures 4 and 5 show the estimated data for total crashes, while Figures 6 and 7 show the estimated data for FI crashes. These graphs enable estimation of the R^2 by severity type (total or FI) and by year, as presented in Table 10.

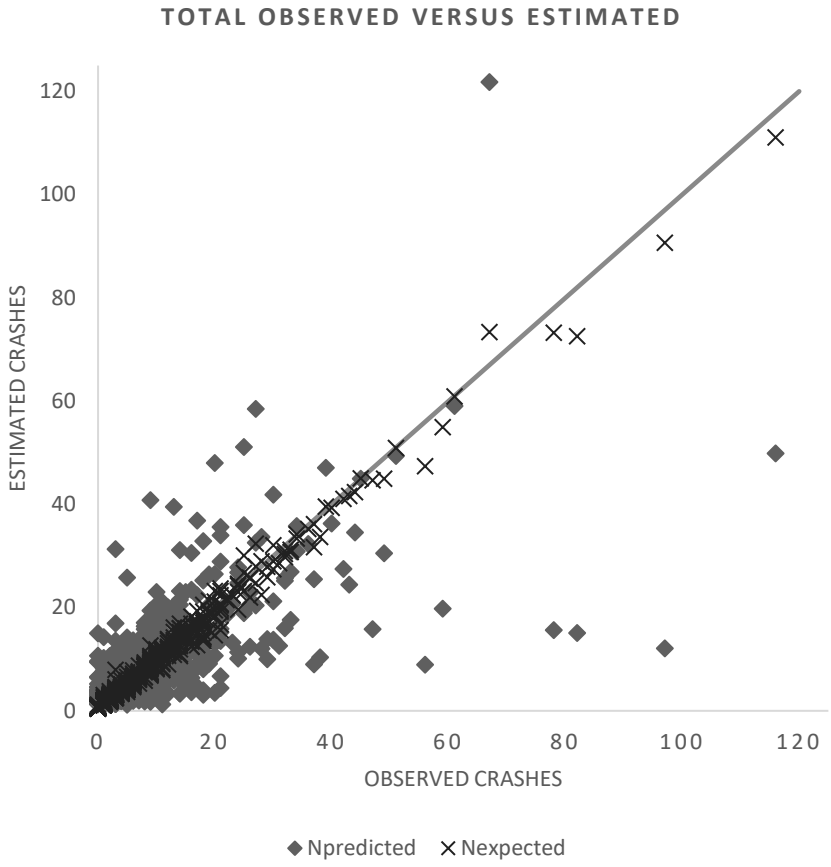

Figure 16 - The correlation between the observed crash data and the estimated calibrated $N_{predicted}$ and $N_{expected}$ for all crashes for all study years.

After applying the EB method, the performance of $N_{expected}$ corroborates the literature studies: the points sit closer to the centerline, which means $N_{expected}$ is very close to $N_{observed}$. On the other hand, $N_{predicted}$ shows a moderate dispersion. The predicted values above the centerline are denser, while the points under the centerline are more dispersed (Figure 17).

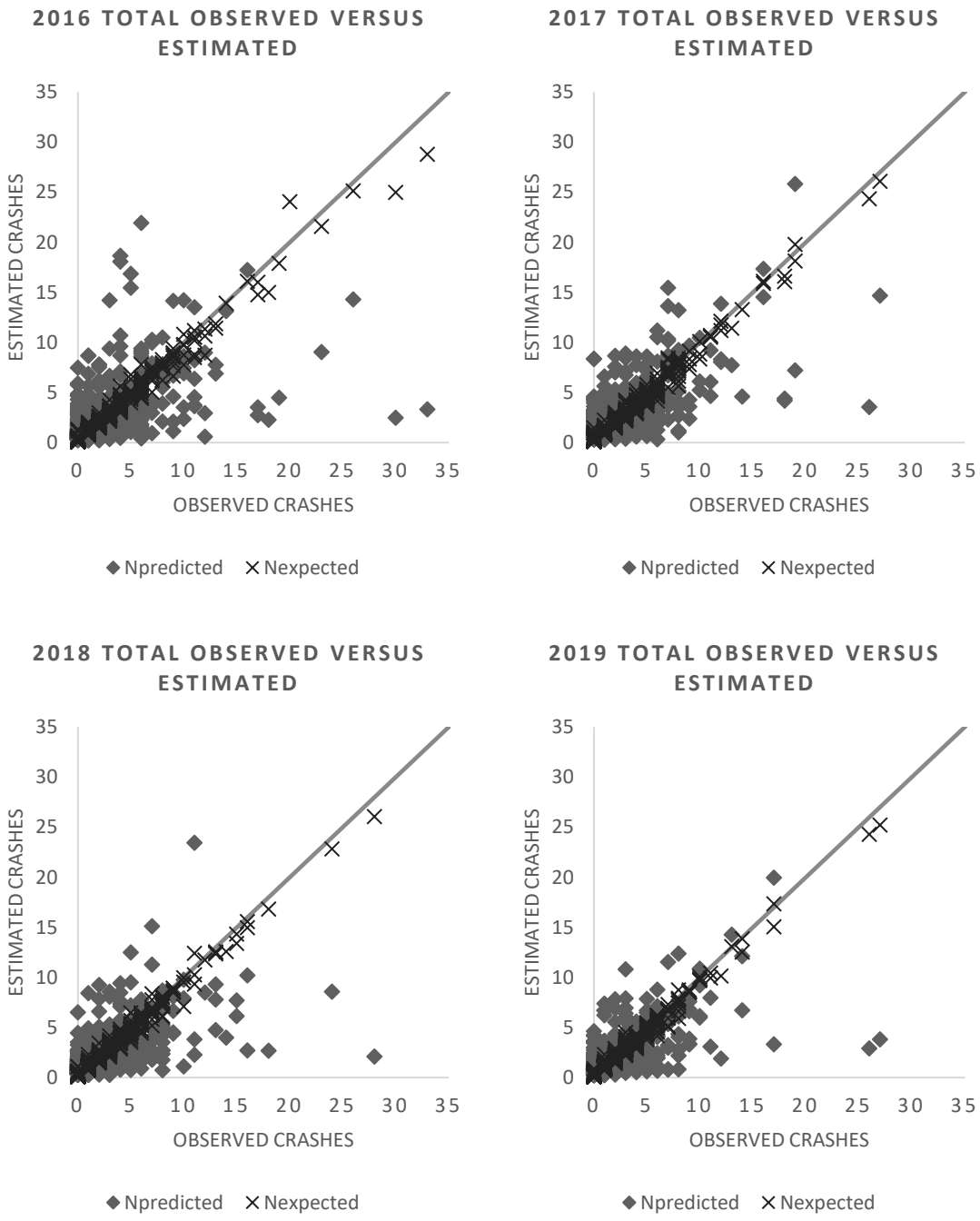

Figure 17 – The correlation between the observed crashes and the estimated calibrated $N_{predicted}$ and $N_{expected}$ for all types of crashes in 2016, 2017, 2018, and 2019.

The graphs for each study year are similar to the one presented in Figure 18. The year 2019 seems to have denser values of $N_{predicted}$, which means that the prediction of 2019 was closer to the actual number of crashes. On the contrary, the estimated values for 2016 seem diffuse.

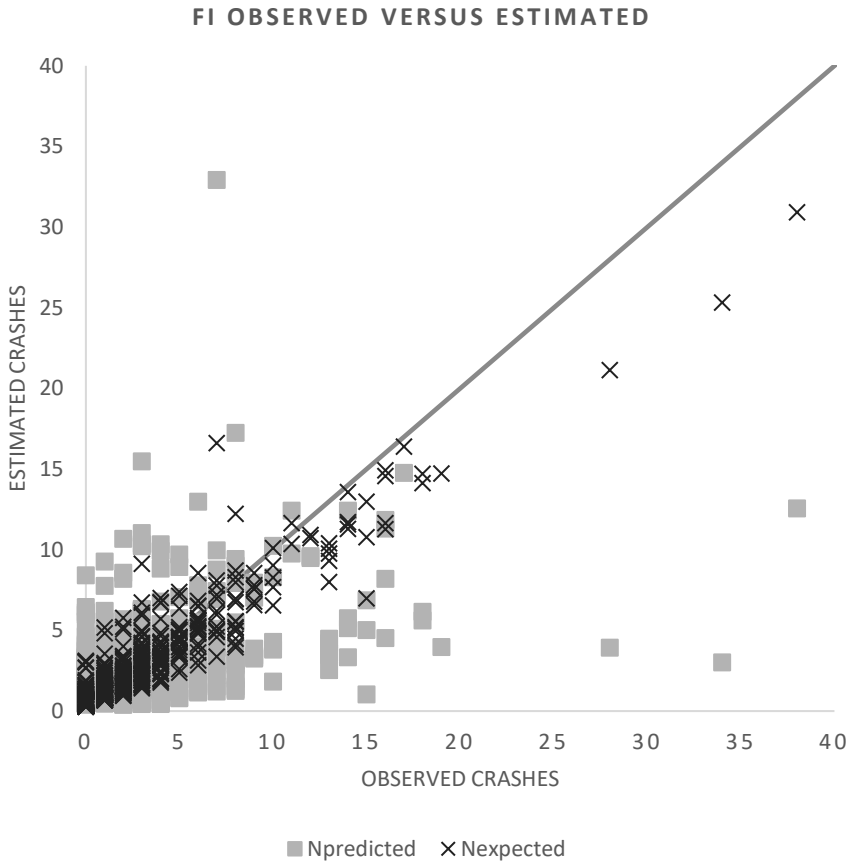

Figure 18 - The correlation between the observed crashes and the estimated calibrated $N_{predicted}$ and $N_{expected}$ for FI crashes at the total period of study.

Since the FI crashes represent a smaller sample, changing the graph scale allows having a clearer perception of the $N_{predicted}$ performance. Again, the predicted values are denser above the centerline than under, implying that the model underpredicted values more often than overpredicted. However, most $N_{expected}$ for FI crashes are under the centerline, meaning that most of the expected values underpredicted the FI observed crashes. Thus, the EB method did not have the same performance as for all types of crashes. Here, the expected crashes are more scattered, and the results indicate underprediction. The performance of $N_{expected}$ in Figure 18 is similar to Figure 19, which means that the EB method underpredicted the observed crash counts. The graphs show that, for each year, the model underestimates the FI crashes in cases where more than five crashes are observed in the segment. Finally, Table 19 presents the R^2 estimated through each developed graph.

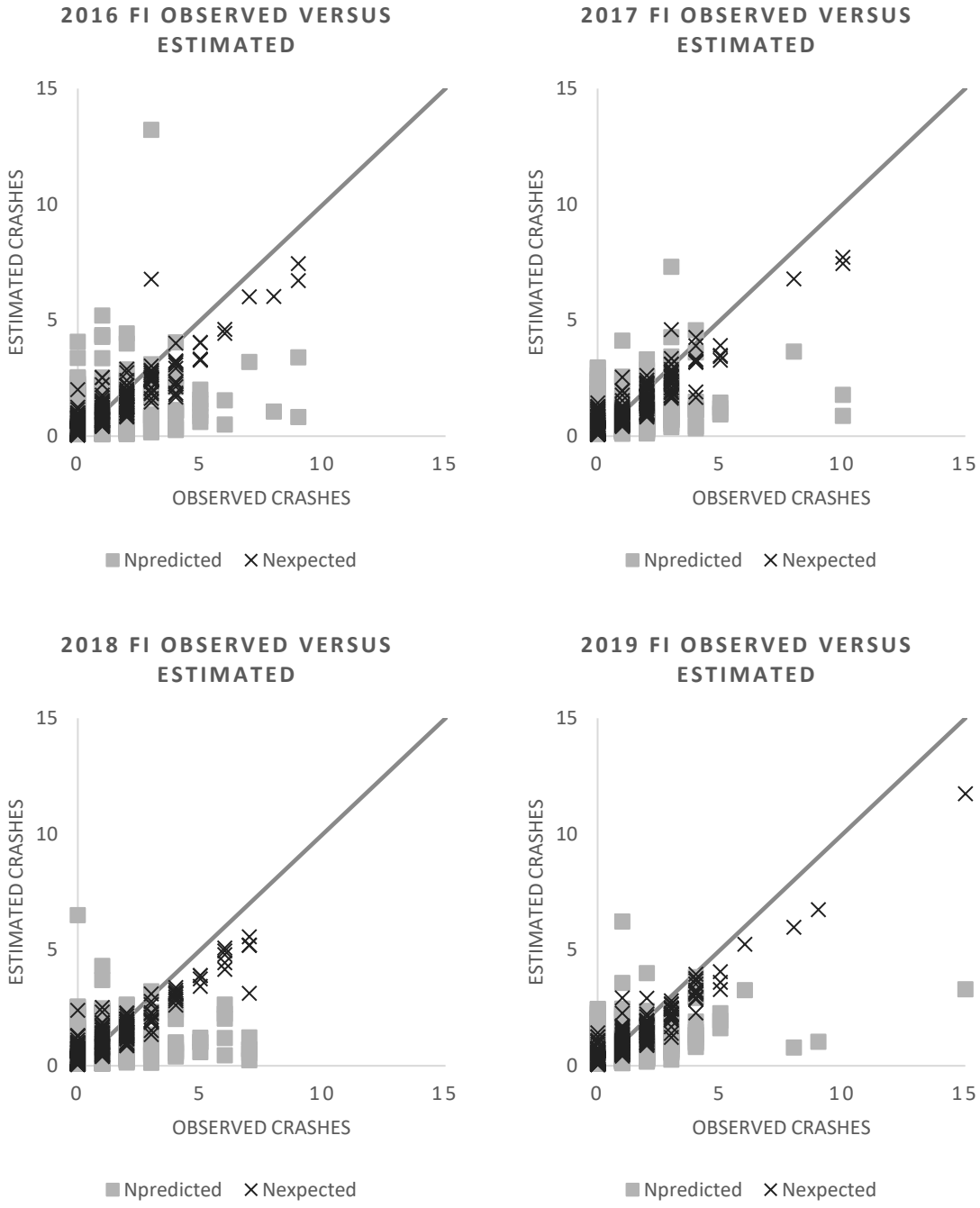

Figure 19 – The correlation between the observed crashes and the estimated calibrated $N_{predicted}$ and $N_{expected}$ for FI crashes in 2016, 2017, 2018, and 2019.

Table 19 - R^2 estimated for $N_{predicted}$ and $N_{expected}$ by year and by severity type

Severity type	**Total**					**FI**				
Year of Study	2016	2017	2018	2019	2016 - 2019	2016	2017	2018	2019	2016 - 2019
Calibrated $N_{predicted}$	0.26	0.43	0.34	0.40	0.45	0.12	0.19	0.10	0.23	0.24
$N_{expected}$	0.98	0.98	0.99	0.99	0.99	0.85	0.87	0.89	0.91	0.88

The value of R^2 is another GOF test result, where a number represents the observed versus estimated graphs. With this, it is possible to compare different scenarios, which could also support assessing the prediction model. Unlike the other GOF tests, the higher the value of R^2, the better because it represents the correlation coefficient. As anticipated, the R^2 for expected crashes is much higher than the predicted ones after applying the EB method because the observed number of crashes is accounted for in the expected number of crashes. Even so, the FI crashes have smaller R^2 than all types (Table 20).

Table 20 - Result of all the GOF tests applied for Calibrated Predicted crashes

Calibrated Predicted Crashes				
Goodness of Fit Test	**MAD**	**MAPE**	**RMSE**	**R^2**
Total	4.44	53%	8.59	0.45
FI	1.92	78%	3.38	0.24

Table 20 shows that MAD and RMSE have lower values using FI crashes, while MAPE and R^2 showed better performance for all crashes.

Table 21 - Result of all the GOF tests applied for Expected crashes

Expected Crashes				
Goodness of Fit Test	**MAD**	**MAPE**	**RMSE**	**R^2**
Total	0.80	10%	1.33	0.99
FI	0.86	35%	1.35	0.88

Table 21, on the other hand, comparing the GOF parameters, presented better results for all types of crashes. That result indicates that the prediction of crashes by the HSM model performed better for all crash types.

This study highlights the importance of obtaining a deeply validated tool to support the financing of projects for road safety improvement, which is why the Highway Safety Manual was chosen. This work obtained Cx=2.62 for the total number

of crashes and Cx=2.34 for FI for the study period from 2016 to 2019, demonstrating that the HSM SPF underestimates the number of crashes for the Brazilian highways or others that are similar. Regarding the decision-making on the severity chosen to develop the predictions, this study's results seem to favor the use of the total number of crashes, even if there is underreporting in some places.

4.3 Crash data analysis for 2020

As 2020 was an atypical year, traffic worldwide was altered by the COVID-19 pandemic. Recent studies still investigate its impact on human health, including traffic-related fatality and injury (Barnes et al., 2022). Figure 20 presents the PDO crashes, and Figure 21 shows the traffic-related fatalities on state highways in 2019, 2020, and 2021 that the government has reported on its website (São Paulo state government, 2022). There is a significant difference in PDO crashes between April 2019 and April 2020, representing a 40% reduction in PDO crash counts. The highest reduction of fatal crashes was also between April 2019 and April 2020, about 27%. Although the lockdown started on March 22nd, 2020, in the state of São Paulo, the impact was more significant in April 2020. The graphs also present the moving average of crashes considering twelve months, showing the crash reduction for that period. The monthly oscillation shows that June and July have a high rate of crashes due to the usual vacation time in Brazil. Even so, the moving average shows that in 2020 the number of crashes in the Southern winter decreased compared to previous months, indicating an unexpected drop, even though it was a holiday and party period in Brazil.

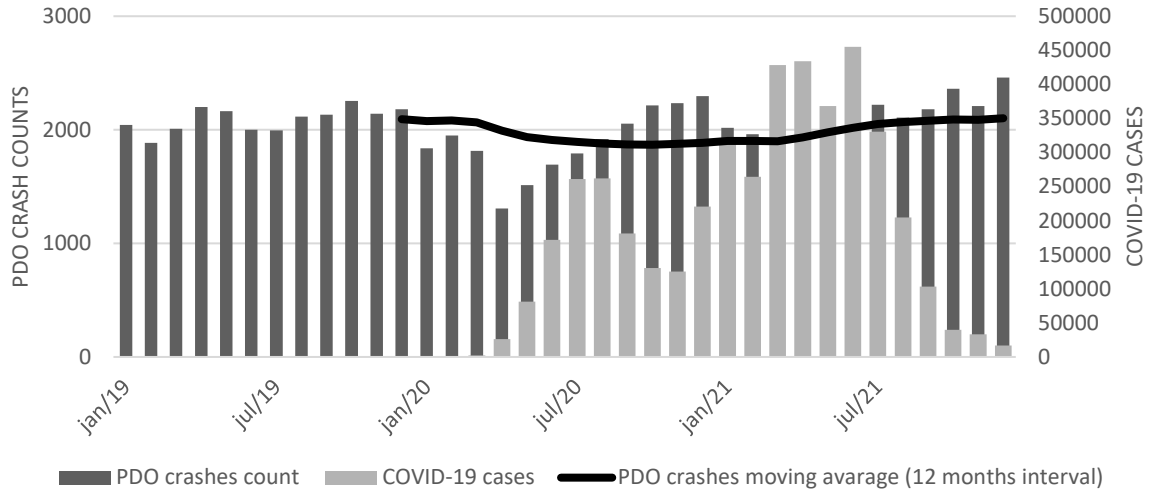

Figure 20 - PDO crashes on state highways in 2019, 2020, and 2021. Source: (São Paulo state government, 2022)

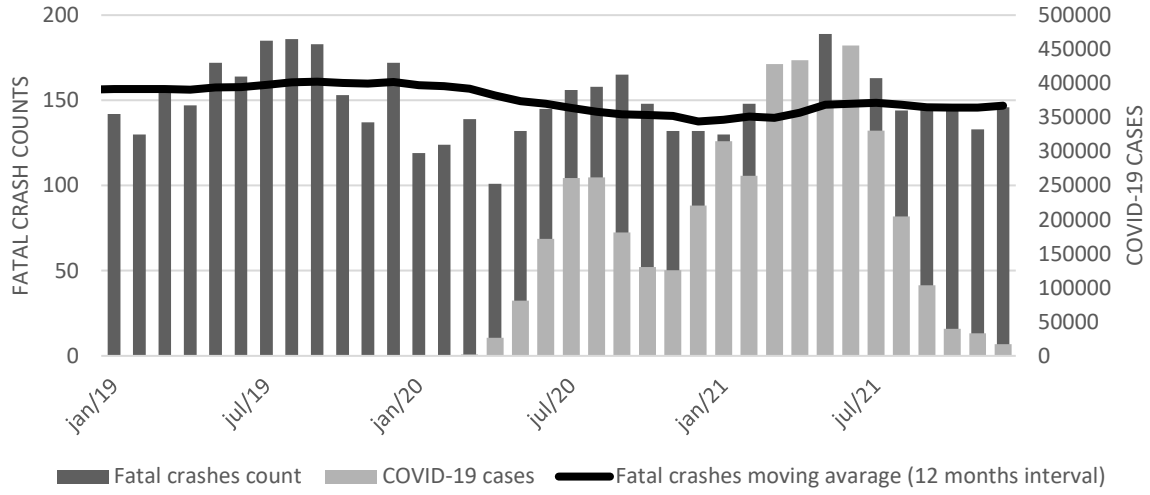

Figure 21 - Fatal crashes on state highways in 2019, 2020, and 2021. Source: (São Paulo state government, 2022).

Table 22 and Figure 22 show the variation of fatal crashes and AADT with the average and the counts of the previous year. The suggestion is that the negative variation of crashes is related to the reduction of AADT caused by the disease control measures at the time.

Table 22 - Comparison of estimated variance in fatalities and AADT on state highways in recent years. Source: (São Paulo state government, 2022).

Year	Fatal Crashes				AADT			
	Count	Mean	% Change compared to		Count	Mean	% Change compared to	
			Previous year	Mean			Previous year	Mean
2015	1872	1836	No data available	2%	No data available	14137	-	-
2016	1853		-1%	1%	14598		-	3%
2017	1911		3%	4%	14149		-3%	0%
2018	1876		-2%	2%	14183		0%	0%
2019	1929		3%	5%	15128		7%	7%
2020	1651		-14%	-10%	12092		-207%	-14%
2021	1763		7%	-4%	16764		39%	19%

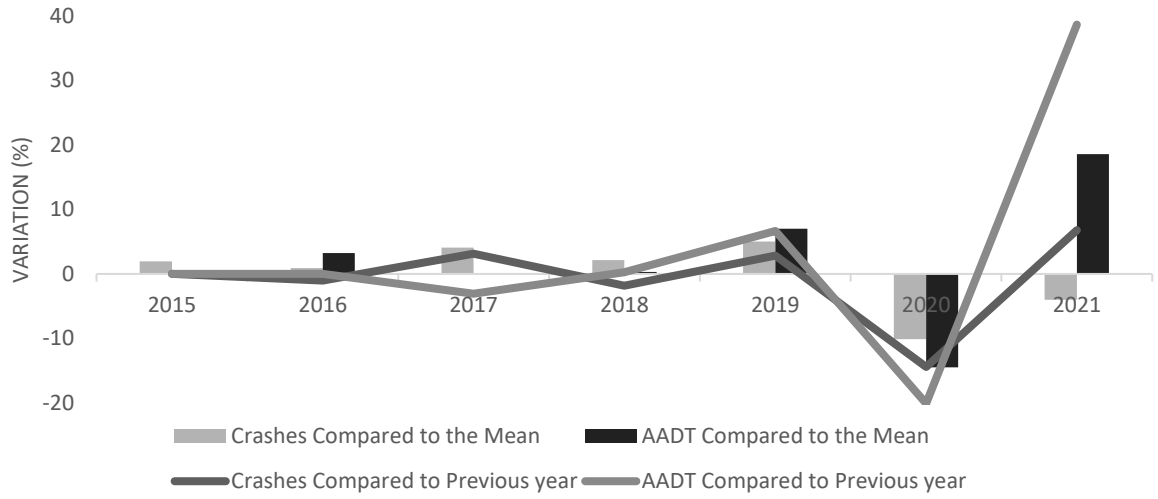

Figure 22 - An estimated variation of crashes and AADT for state highways. Source: (São Paulo state government, 2022).

Thus, to explore the impact of COVID-19 on the studied segments, the crash data from 2020 are presented in Table 23. The decrease in crashes in 2020 compared to the average of the previous four years (1,487 all types and 435 FI crashes) is about 20% and 11% for all types of crashes and FI crashes, respectively.

Table 23 - Main aspects related to crash data from 2016, 2017, 2018, 2019, and 2020.

Severity type	**Total**					**FI**				
Year of Study	2016	2017	2018	2019	**2020**	2016	2017	2018	2019	**2020**
∑	1653	1597	1398	1301	**1182**	451	467	406	415	**389**
Mean	2.32	2.24	1.96	1.83	**1.66**	0.63	0.66	0.57	0.58	**0.55**
Standard Deviation	3.47	3.08	2.94	3.08	**2.73**	1.18	1.13	1.13	1.17	**1.13**
Max	33	27	28	39	**27**	9	10	7	15	**11**
Min	0	0	0	0	**0**	0	0	0	0	**0**

The 2020 AADT data allowed the crash prediction for 2020 since the HSM prediction model is based on AADT values and segment length. Therefore, the calibration factors obtained and presented in section 4.1 ($C_{x,\ TOTAL}$=2.62, and $C_{x,\ FI}$=2.35) were used to calculate the calibrated $N_{predicted}$ (Table 24). The four previous years' data was the baseline to obtain the parameters used to apply the EB method, allowing the calculation to obtain the $N_{expected}$ as well.

Table 24 - HSM prediction model estimation compared to observed crashes.

	Severity	**2016**	**2017**	**2018**	**2019**	**Four-years mean**	**2020**
Observed Crashes	Total	1653	1597	1398	1301	1487	**1182**
	FI	451	467	406	415	435	**389**
Predicted Crashes ($N_{predicted}$)	Total	565	570	545	587	567	**498**
	FI	182	186	181	191	185	**164**
Calibrated Predicted Crashes (Cal. $N_{predicted}$)	Total	-	-	-	-	-	**1308**
	FI	-	-	-	-	-	**386**
Expected Crashes (EB) ($N_{expected}$)	Total	1622	1581	1402	1298	1476	**1205**
	FI	457	472	420	422	443	**394**

Since the AADT has also changed due to the COVID-19 pandemic, the N_{spf} reflects the impact of the pandemic. Nevertheless, the $N_{observed}$ is still about 10% lower than the calibrated $N_{predicted}$ for all types of crashes. On the other hand, the calibrated prediction of FI crashes is highly close to the observed counts. Besides, the influence of the observed number of crashes through the EB method application influences the $N_{expected}$ to be closer to $N_{observed}$. This could indicate that the model performs well in predicting unseen data.

Table 25 shows that for MAD and RMSE, the FI demonstrates a better model adjustment to the actual inputs. On the other hand, the MAPE and R^2 indicate that using all types of crashes has succeeded in the model adjustment. The high MAPE value for 2020 is explained due to the sudden reduction of crashes, while the model was based on the previous years.

Table 25 - Result of all the GOF tests applied for Calibrated Predicted crashes.

Calibrated Predicted Crashes				
Goodness of Fit Test	**MAD**	**MAPE**	**RMSE**	**R^2**
Total (4 years)	4.44	53%	8.59	0.45
FI (4 years)	1.92	78%	3.38	0.24
Total (2020)	1.33	80%	2.30	0.32
FI (2020)	0.62	114%	1.04	0.17

GOF tests applied after the EB application, including the 2020 data, show that the model performs better using all types of crashes (Table 26). While further investigation is needed to understand the influence of infection prevention and control procedures on Brazilian road safety, some numbers, such as the reduction in crash counts shown in Table 13, suggest that some change has occurred. The reduction of around 14% in fatal crashes in 2020 compared to 2019 and around 10% compared to the average of the last five years presents a very different scenario for road safety analysis. Therefore, the need for a model that predicts the crash counts based on road geometry and AADT, being a reliable tool even for atypical moments, was the main reason for testing the use of the HSM prediction model for this unusual period.

Table 26 - Result of all the GOF tests applied for expected crashes.

Expected Crashes				
Goodness of Fit Test	**MAD**	**MAPE**	**RMSE**	**R^2**
Total (4 years)	0.80	10%	1.33	0.99
FI (4 years)	0.86	35%	1.35	0.88
Total (2020)	0.24	15%	0.37	0.98
FI (2020)	0.29	52%	0.44	0.90

5 CONCLUSIONS

The HSM is an essential source for quantitative crash analysis and evaluation. The estimation of crash frequency by HSM methodology is a tool to facilitate decision-making based on Safety Performance Functions (SPFs). Because HSM's SPFs are regression models developed for other areas, it requires calibration to modify the SPFs for local use.

Applying the HSM predictive method for different jurisdictions needs caution. It demands further investigation into roadway systems, driver training and behavior, and crash frequency and patterns that vary from the conditions in which it was developed. Thus, whenever data is available, the HSM recommends agencies and researchers either develop local SPFs or calibrate HSM-based SPFs to local conditions to improve the success of crash frequency estimation.

This study intended to assess results from HSM crash prediction model deployment for multilane rural highway segments in the most inhabited state in Brazil. The HSM prediction procedure was used to estimate the local calibration factors (C_x).

In 2015, the crash reporting system changed in Brazil. Collisions with Property Damage Only (PDO), which would be reported by the road police themselves, could then be reported online, leading to underreporting of accidents across the country. Due to this problem, the HSM predictive model was applied for total and fatal and injury severity (FI) of crashes.

The C_x obtained in Brazil was calculated for heterogeneous segments in Brazil. This study obtained C_x=2.62 for all types of crashes and C_x=2.35 for FI crashes, showing similarities to Waihrich & Andrade (2015), which found Cx=2.37 for the same facility type in the state of Minas Gerais. The studies based on Brazilian crash data concluded that the HSM predictive models usually underestimate the number of crashes in Brazilian facilities.

The goodness of fit (GOF) measures were employed after the calibration procedure to measure whether the predicted and expected crashes would represent a well-fitted. The performance metrics applied in this study were MAD, MAPE, RMSE, R^2, and observed versus estimated crash graphs separately for all types of crashes and for the crashes in which someone got killed or injured (FI).

It is relevant to note that Brazilian data is generally not always easy to obtain, and multiple heterogeneous variables make it difficult to generate SPFs valid for the entire

country. Thus, to analyze the model's performance for Brazilian conditions, it is essential to establish some thresholds to determine a "good-enough" approach. Applying a calibrated version can bring insights into a data-driven approach that would be impossible if it were not for the HSM equations. In this way, utilizing the EB method is even more beneficial.

As expected, after applying the EB method, the estimated values fit the data quite well. The MAD, MAPE, and RMSE show that models for all types of crashes perform better than FI crashes. On the other hand, the values found for MAD and RMSE indicate that the variation of calibrated predicted values is more remarkable when including PDO crashes. This is reasonable since FI crashes represent a smaller sample (about only 30% of the total crash data). The MAD for FI crashes was about 43% of MAD for total crashes, while for RMSE, this proportion was about 39%. Besides, Andrade (2015) found 5.54 MAD for total crashes at Minas Gerais, which is 24% greater than the MAD value found for total crashes at São Paulo (MAD=4.44).

On the other hand, the graphs allowed us to assess the model's performance. The $N_{expected}$, after application of the EB method, follows the expectation: the points are following the centerline, which means the $N_{expected}$ is very close to the $N_{observed}$. After that, $N_{predicted}$ shows a supposed dispersion. The predicted values above the centerline are denser, while the points under the centerline are more diffuse.

Comparing the GOF parameters, most of them presented better results for the prediction using all types of crashes, which indicates that the underreporting of crashes does not affect model validity. However, it may have a minor impact on the absolute numbers.

Finally, as 2020 was an atypical year in which the COVID-19 pandemic altered traffic around the world, this study aimed to assess the application of the calibrated prediction model to a sudden disturbance in traffic behavior. Unlike studies that investigated how COVID-19 changed road safety in general, this work aimed to analyze the model's performance during the pandemic year 2020. In that year, a significant reduction in AADT occurred, including the exact locations where the SPFs were calibrated. The HSM method was applied to 2020 using the C_x obtained from the four previous years. For 2020, the $N_{observed}$ was lower than the calibrated $N_{predicted}$ for all types of crashes. This finding might indicate that additional risk factors not addressed by SPF play a role in safety performance. The calibrated prediction of FI crashes was very close to the observed counts, which expresses the model's reliability.

As the HSM recommends the calibration process, this work can be seen as a reference for the Brazilian rural multilane safety assessment. The result of this study can be used by highway administration, municipalities, and toll agencies for practical safety assessment and guidance by applying the HSM's SPFs. It can also be a tool to support resource prospecting for the implementation of appropriate countermeasures to increase road safety.

Besides that, the findings of this work are expected to be a reference for researchers who want to understand the transferability of SPFs in a context other than the HSM development, showing the different performance results of the model using different severities, and applied to this recent atypical year in worldwide.

The localization aggregation process impacted the HSM SPF calibration procedure. Hence, it is suggested that future studies may use calibration functions and different calibration methods to improve the accuracy of crash prediction when developing a model is not feasible. Since the calibration is a function of the variables and not only a single factor obtained by the ratio of observed and predicted values, it usually improves the calculated results, even though it requires the particular expertise of the analyst.

Other GOFs, such as cure plots, chi-square, and coefficient of variation, may be used to assess the adequacy of the calibration process. The application of the GOF tests must also have limits to measure what is considered a good model and whether the model should be applied depending on its parameters. Future studies focusing on jurisdiction-specific SPFs development for local conditions are desirable. Likewise, some additional questions about the frequency of SPF calibration and temporal transferability can bring more insights into this research topic in the future.

6 REFERENCES

AASHTO. (2010). *Highway Safety Manual* (Vol. 1).

Abdel-Aty, M. A., & Radwan, A. E. (2000). Modeling traffic accident occurrence and involvement. *Accident Analysis and Prevention*. https://doi.org/10.1016/S0001-4575(99)00094-9

Al-Ahmadi, H. M., Jamal, A., Ahmed, T., Rahman, M. T., Reza, I., & Farooq, D. (2021). Calibrating the Highway Safety Manual Predictive Models for Multilane Rural Highway Segments in Saudi Arabia. *Arabian Journal for Science and Engineering*, *46*(11), 11471–11485. https://doi.org/10.1007/s13369-021-05944-6

Aljanahi, A. A. M., Rhodes, A. H., & Metcalfe, A. v. (1999). Speed, speed limits, and road traffic accidents under free flow conditions. In *Accident Analysis and Prevention* (Vol. 31).

Andrade, G. R. de, & Setti, J. R. (2011). Método para Caracterização e Classificação de Trechos Homogêneos Rodoviários. *VII Congresso Brasileiro de Rodovias e Concessões*.

Barbosa, H., Cunto, F., Bezerra, B., Nodari, C., & Jacques, M. A. (2014). Safety performance models for urban intersections in Brazil. *Accident Analysis and Prevention*, *70*, 258–266. https://doi.org/10.1016/j.aap.2014.04.008

Barnes, S. R., Beland, L. P., Huh, J., & Kim, D. (2022). COVID-19 lockdown and traffic accidents: Lessons from the pandemic. *Contemporary Economic Policy*, *40*(2), 349–368. https://doi.org/10.1111/coep.12562

Brazil Ministry of Justice and Public Security. (2015). *PRF disponibiliza serviço via internet para registro de acidentes sem vítimas*. Government Official Website. https://www.justica.gov.br/news/prf-disponibiliza-servico-via-internet-para-registro-de-acidentes-sem-vitimas

Buyco, C., & Saccomanno, F. F. (1988). Analysis of truck accident rates using loglinear models. *Canadian Journal of Civil Engineering*, *15*(3), 397–408. https://doi.org/10.1139/l88-055

Ceder, A., & Livneh, M. (1982). Relationships between road accidents and hourly traffic flow-I. Analyses and interpretation. *Accident Analysis and Prevention*. https://doi.org/10.1016/0001-4575(82)90004-5

Chang, L.-Y., & Mannering, F. (1999). Analysis of injury severity and vehicle occupancy in truck-and non-truck-involved accidents. In *Accident Analysis and Prevention* (Vol. 31). www.elsevier.com/locate/aap

Charnes, A., Cooper, W. W., Seiford, L., & Stutz, J. (1982). A multiplicative model for efficiency analysis. *Socio-Economic Planning Sciences*, *16*(5), 223–224. https://doi.org/10.1016/0038-0121(82)90029-5

Confederação Nacional do Transporte. (2020). Anuário CNT do Transporte 2020 - Estatísticas consolidadas. In *Cnt*. http://anuariodotransporte.cnt.org.br

Cunto, F., Sobreira, L., & Ferreira, S. (2015). Assessing the transferability of the highway safety manual predictive method for urban roads in Fortaleza City, Brazil. *Journal of Transportation Engineering*, *141*(1). https://doi.org/10.1061/(ASCE)TE.1943-5436.0000734

Dadvar, S., Lee, Y. J., & Shin, H. S. (2020). Improving crash predictability of the Highway Safety Manual through optimizing local calibration process. *Accident Analysis and Prevention*, *136*(December 2019), 105393. https://doi.org/10.1016/j.aap.2019.105393

D'Agostino, C. (2014). Investigating transferability and goodness of fit of two different approaches of segmentation and model form for estimating safety performance of motorways. *Procedia Engineering*, *84*, 613–623. https://doi.org/10.1016/j.proeng.2014.10.478

DATASUS. (2020). *Observatório Nacional de Segurança Viária*. https://www.onsv.org.br/

de Andrade, F. R., & Antunes, J. L. F. (2019). Trends in the number of traffic accident victims on Brazil's federal highways before and after the start of the Decade of Action for Road Safety. *Reports in Public Health*, *35*(8), 1–11. https://doi.org/10.1590/0102-311X00250218

Dong, N., Zhang, J., Liu, X., Xu, P., Wu, Y., & Wu, H. (2022). Association of human mobility with road crashes for pandemic-ready safer mobility: A New York City case study. *Accident Analysis and Prevention*, *165*. https://doi.org/10.1016/j.aap.2021.106478

Dong, X., Xie, K., & Yang, H. (2022). How did COVID-19 impact driving behaviors and crash Severity? A multigroup structural equation modeling. *Accident Analysis & Prevention*, *172*, 106687. https://doi.org/10.1016/j.aap.2022.106687

Ebrahim Shaik, Md., & Ahmed, S. (2022). An overview of the impact of COVID-19 on road traffic safety and travel behavior. *Transportation Engineering*, *9*, 100119. https://doi.org/10.1016/j.treng.2022.100119

Elagamy, S. R., El-Badawy, S. M., Shwaly, S. A., Zidan, Z. M., & Shahdah, U. E. (2020). Segmentation effect on the transferability of international safety performance functions for rural roads in Egypt. *Safety*, *6*(3), 1–24. https://doi.org/10.3390/SAFETY6030043

Elvik, R. (2007). *State-of-the-art approaches to road accident black spot management and safety analysis of road networks* (p. 126). National Research Council of Norway. https://www.toi.no/getfile.php/139022/Publikasjoner/TØI rapporter/2007/883-2007/883-2007-nett.pdf

Farid, A., Abdel-Aty, M., & Lee, J. (2019). Comparative analysis of multiple techniques for developing and transferring safety performance functions. *Accident Analysis and Prevention*, *122*(September 2018), 85–98. https://doi.org/10.1016/j.aap.2018.09.024

Farid, A., Abdel-Aty, M., Lee, J., Eluru, N., & Wang, J. H. (2016). Exploring the transferability of safety performance functions. *Accident Analysis and Prevention*, *94*, 143–152. https://doi.org/10.1016/j.aap.2016.04.031

Feng, M., Wang, X., Lee, J., Abdel-Aty, M., & Mao, S. (2020). Transferability of safety performance functions and hotspot identification for freeways of the United States and China. *Accident Analysis & Prevention*, *139*(January), 105493. https://doi.org/10.1016/j.aap.2020.105493

Foldvary, L. A. (1979). Road accident involvement per miles travelled-V. *Accident Analysis and Prevention*, *11*(2), 75–99. https://doi.org/10.1016/0001-4575(79)90017-4

Geurts, K., & Wets, G. (2003). Black Spot Analysis Methods : Literature Review. *Onderzoekslijn Kennis Verkeersonveiligheid*, *1*(Black Spot), 32.

Hauer, E. (2004). Statistical road safety modeling. *Transportation Research Record*, *1897*, 81–87. https://doi.org/10.3141/1897-11

Hauer, E. (2015). The Art of Regression Modeling in Road Safety. In *The Art of Regression Modeling in Road Safety*. Springer International Publishing. https://doi.org/10.1007/978-3-319-12529-9

Hauer, E., Bonneson, J., Council, F., Srinivasan, R., & Zegeer, C. (2012). Crash modification factors. *Transportation Research Record*, *2279*, 67–74. https://doi.org/10.3141/2279-08

Hydén, C., & Várhelyi, A. (2000). The effects on safety, time consumption and environment of large scale use of roundabouts in an urban area: a case study. In *Accident Analysis and Prevention* (Vol. 32). www.elsevier.com/locate/aap

Ivan, J. N., Pasupathy, R. K., & Ossenbruggen, P. J. (1999). Differences in causality factors for single and multi-vehicle crashes on two-lane roads. In *Accident Analysis and Prevention* (Vol. 31). www.elsevier.com/locate/aap

Jovanis, P. P., & Chang, H. L. (1986). Modeling the Relationship of Accidents To Miles Traveled. *Transportation Research Record*, *1068*, 42–51.

la Torre, F., Meocci, M., Domenichini, L., Branzi, V., Tanzi, N., & Paliotto, A. (2019). Development of an accident prediction model for Italian freeways. *Accident Analysis and Prevention*, *124*(December 2018), 1–11. https://doi.org/10.1016/j.aap.2018.12.023

Li, J., & Zhao, Z. (2022). Impact of COVID-19 travel-restriction policies on road traffic accident patterns with emphasis on cyclists: A case study of New York City. *Accident Analysis and Prevention*, *167*. https://doi.org/10.1016/j.aap.2022.106586

Li, L., Gayah, V. v., & Donnell, E. T. (2017). Development of regionalized SPFs for two-lane rural roads in Pennsylvania. *Accident Analysis and Prevention*, *108*(September), 343–353. https://doi.org/10.1016/j.aap.2017.08.035

Lord, D., & Miranda-Moreno, L. F. (2008). Effects of low sample mean values and small sample size on the estimation of the fixed dispersion parameter of Poisson-gamma models for modeling motor vehicle crashes: A Bayesian perspective. *Safety Science*. https://doi.org/10.1016/j.ssci.2007.03.005

Matarage, I. C., & Dissanayake, S. (2020). Quality assessment between calibrated highway safety manual safety performance functions and calibration functions for predicting crashes on freeway facilities. *Journal of Traffic and Transportation Engineering (English Edition)*, *7*(1), 76–87. https://doi.org/10.1016/j.jtte.2019.12.001

Miaou, S. P. (1994). The relationship between truck accidents and geometric design of road sections: Poisson versus negative binomial regressions. *Accident Analysis and Prevention*, *26*(4), 471–482. https://doi.org/10.1016/0001-4575(94)90038-8

Miaou, S. P., & Lord, D. (2003). Modeling Traffic Crash-Flow Relationships for Intersections: Dispersion Parameter, Functional Form, and Bayes Versus Empirical Bayes Methods. *Transportation Research Record*, *1840*, 31–40. https://doi.org/10.3141/1840-04

Oppe, S. (1979). The use of multiplicative models for analysis of road safety data. *Accident Analysis and Prevention*, *11*(2), 101–115. https://doi.org/10.1016/0001-4575(79)90018-6

Quddus, M. A. (2008). Time series count data models: An empirical application to traffic accidents. *Accident Analysis and Prevention*. https://doi.org/10.1016/j.aap.2008.06.011

Sao Paulo state government. (2022). *Informapa SP*. http://www.respeitoavida.sp.gov.br/relatorios/

Silva, K. C. R. (2012). *Aplicação do modelo de previsão de acidentes do HSM em rodovias de pista simples do Estado de São Paulo* [Universidade de São Paulo]. https://doi.org/10.11606/D.18.2012.tde-15022012-172539

Silva, K. C. R. (2017). *Assessing the transferability of crash prediction models for two lane highways in Brazil* [Universidade de São Paulo]. https://doi.org/10.11606/T.18.2017.tde-10112017-215500

Srinivasan, R., Colety, M., Bahar, G., Crowther, B., & Farmen, M. (2016). Estimation of calibration functions for predicting crashes on rural two-lane roads in Arizona. *Transportation Research Record*, *2583*(2583), 17–24. https://doi.org/10.3141/2583-03

Sun, C., Brown, H., Edara, P., Carlos, B., & Nam, K. (2013). Calibration of the Highway Safety Manual for Missouri. *Final Reports & Technical Briefs from Mid-America Transportation Center. Paper 94.*, 1–240.

Vanlaar, W. G. M., Woods-Fry, H., Barrett, H., Lyon, C., Brown, S., Wicklund, C., & Robertson, R. D. (2021). The impact of COVID-19 on road safety in Canada and the United States. *Accident Analysis and Prevention*, *160*. https://doi.org/10.1016/j.aap.2021.106324

Waihrich, D. R. L. da S., & Andrade, M. (2015). Calibração do método de previsão de acidentes do Highway Safety Manual (HSM) para trechos rodoviários de pista dupla no Brasil. *Xxix Congresso Nacional De Pesquisa Em Transporte Da Anpet*, *Ouro Preto*, 1434–1437.

World Health Organization. (2018). *Global status report on road safety 2018* (p. 424). https://www.who.int/violence_injury_prevention/road_safety_status/2018/en/

Wright, C. C., Abbess, C. R., & Jarrett, D. F. (1986). Estimating the regression-to-mean effect associated with road accident black spot treatment: Towards a more realistic approach. *Accidents Analysis and Prevention*, *20*(3), 199–214.

Yao, Y., Geara, T. G., & Shi, W. (2021). Impact of COVID-19 on city-scale transportation and safety: An early experience from Detroit. *Smart Health*, *22*. https://doi.org/10.1016/j.smhl.2021.100218

Yasin, Y. J., Grivna, M., & Abu-Zidan, F. M. (2021). Global impact of COVID-19 pandemic on road traffic collisions. In *World Journal of Emergency Surgery* (Vol. 16, Issue 1). BioMed Central Ltd. https://doi.org/10.1186/s13017-021-00395-8

Yehia, A., Wang, X., Feng, M., Yang, X., Gong, J., & Zhu, Z. (2021). Applicability of boosting techniques in calibrating safety performance functions for freeways. *Accident Analysis and Prevention*, *159*. https://doi.org/10.1016/j.aap.2021.106193